State of Alaska Department of Transportation and Public Facilities

THERMOSYPHON DEVICES AND SLAB-ON-GRADE FOUNDATION DESIGN

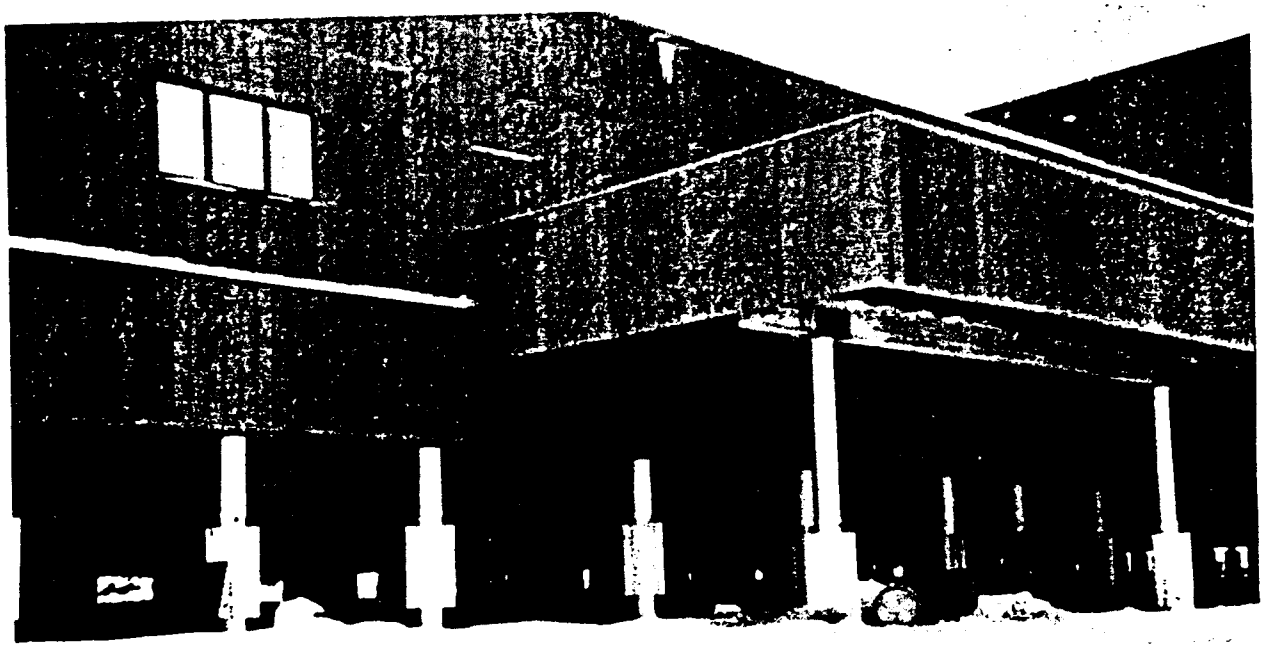

Report No. AK-RD-86-16

Cover Photo:

Galena School

Photo Courtesy of

Erwin L. Long

E85.23

FINAL REPORT

THERMOSYPHON DEVICES AND SLAB-ON-GRADE FOUNDATION DESIGN

by

John P. Zarling
Institute of Water Resources/Engineering Experiment Station
University of Alaska
Fairbanks, Alaska 99775-1760

and

F. Donald Haynes
Cold Regions Research and Engineering Laboratory
Hanover, New Hampshire

June 1985

Prepared for:

STATE OF ALASKA
DEPARTMENT OF TRANSPORTATION AND PUBLIC FACILITIES
RESEARCH SECTION
2301 Peger Road
Fairbanks, Alaska 99701

TABLE OF CONTENTS

LIST OF FIGURES

LIST OF FIGURES (Continued

LIST OF TABLES

ABSTRACT

Subgrade cooling methods to prevent thermal degradation of permafrost in cold regions include the use of thermosyphons with inclined evaporator sections. This laboratory study was conducted to determine the thermal performance characteristics of two commercially available thermosyphons. Evaporator inclination angles ranged from 0° to 12° from the horizontal, and air speeds ranged from 0 to 13.4 miles per hour over the finned condenser sections.

Two standard full size thermosyphons, one charged with CO_2, carbon dioxide and the other with NH_3, anhydrous ammonia, were tested in CRREL's atmospheric wind tunnel. Empirical expressions are presented for heat removal rates as a function of air speed, ambient air temperature and evaporator inclination angle.

An analytical method is also presented to approximate thermal design of foundations using thermosyphons under buildings with a slab-on-grade. We present heat gains from the slab and pad to the thermosyphon as well as the evaporator temperature as functions of time.

NOMENCLATURE

A_o = amplitude of annual air temperature variation, F°
a = outside radius of thermosyphon tube, ft
α = thermal diffusivity of permafrost, ft^2/day
α_s = solar absorptivity
B = exposure factor
C = thermosyphon conductance, Btu/hr-ft-F°
C' = volumetric specific heat of thawed gravel, Btu/ft^3-F°
d_c = thickness of concrete slab, ft
d_i = thickness of insulation, ft
d_f = thickness of fill, ft
d_p = thickness of pad, ft
ε = infrared emissivity
h = convective heat transfer coefficient, Btu/hr-ft^2-F°
h_r = radiative heat transfer coefficient, Btu/hr-ft^2-F°
h_e = evaporative heat transfer coefficient, Btu/hr-ft^2-F°
h_c = condensing heat transfer coefficient, Btu/hr-ft^2-F°
K_p = thermal conductivity of pipe, Btu/hr-ft-F°
K = air-side total conductance, Btu/hr-ft^2-F°
K_c = thermal conductivity of concrete, Btu/hr-ft-F°
K_i = thermal conductivity of insulation, Btu/hr-ft-F°
K_f = thermal conductivity of gravel fill, Btu/hr-ft-F°
K_p = thermal conductivity of gravel pad, Btu/hr-ft-F°
K_g = thermal conductivity of gravel, Btu/hr-ft-F°
K_{pf} = thermal conductivity of permafrost, Btu/hr-ft-F°
L = volumetric latent heat of gravel, Btu/ft^3
P = perimeter, ft
Q = heat flow rate, Btu/hr
R^2 = correlation coefficient
r'_f = radius of freezing front, ft
R_c = thermal resistance of concrete slab, (ft^2-F°-hr)/Btu
R_i = thermal resistance of insulation, (ft^2-F°-hr)/Btu
R_f = thermal resistance of gravel fill, (ft^2-F°-hr)/Btu
R_p = thermal resistance of pad, (ft^2-F°-hr)/Btu
S = spacing between thermosyphons, ft

NOMENCLATURE (Continued)

Ste	=	Stefan number
t	=	time
ΔT	=	temperature difference between the test pipe fluid and air, F°
$\Delta T'$	=	temperature between top of gravel pad and freezing, F°
ΔT^*	=	temperature difference between freezing and average thermosyphon evaporator temperature, °F
T_a	=	ambient air temperature, °F
T_f	=	freezing temperature, °F
T_m	=	mean annual air temperature, °F
T_s	=	floor temperature of building, °F
V	=	wind speed, mi/hr

INTRODUCTION

A two-phase thermosyphon is a device with a very high thermal conductance due to the continuous evaporation and condensation of its working fluid. Thermosyphons have proved successful in a variety of foundation stabilization applications in regions of continuous and discontinuous permafrost.

The heat transfer processes that occur in a thermosyphon are shown in Figure 1. Heat transferred from the ground to the liquid in the evaporator section causes the liquid to evaporate. This vapor then flows from the evaporator section to the condenser section due to a pressure gradient setup by the decrease in the saturation vapor pressure in the condenser section due to its lower temperature. When the vapor contacts the cold surface of the condenser section, a condensate film is formed that returns to the evaporator by gravitational force. The latent heat of vaporization required to evaporate the liquid and, subsequently, released during condensation of the vapor gives rise to the extremely high heat transfer conductances characteristic of the two-phase thermosyphon.

A similar device, referred to as a heat pipe (Feldman, 1967), has a wick structure so that the condensate may return to the evaporator by capillary forces. This allows a heat pipe to transfer heat in the absence of gravity or to transfer heat against gravity (i.e., having the condensing section below the evaporating section where the liquid flows upward through the wick). A wickless heat pipe is generally called a thermosyphon.

There is considerable interest in using thermosyphons for subgrade cooling in permafrost regions. Foundations of this type include gravel fill over undisturbed permafrost, with a layer of insulation separating the concrete floor slab from the fill. The evaporator section of the thermosyphons are placed in the gravel fill anywhere from 8 to 16 feet on center depending upon the design. Evaporator sections have exceeded 190 feet in length for some applications. Slopes of the evaporators are typically 6° (1:10) from the horizontal. However, very few test data exist describing the performance of thermosyphons with a tilted evaporator and vertical condenser.

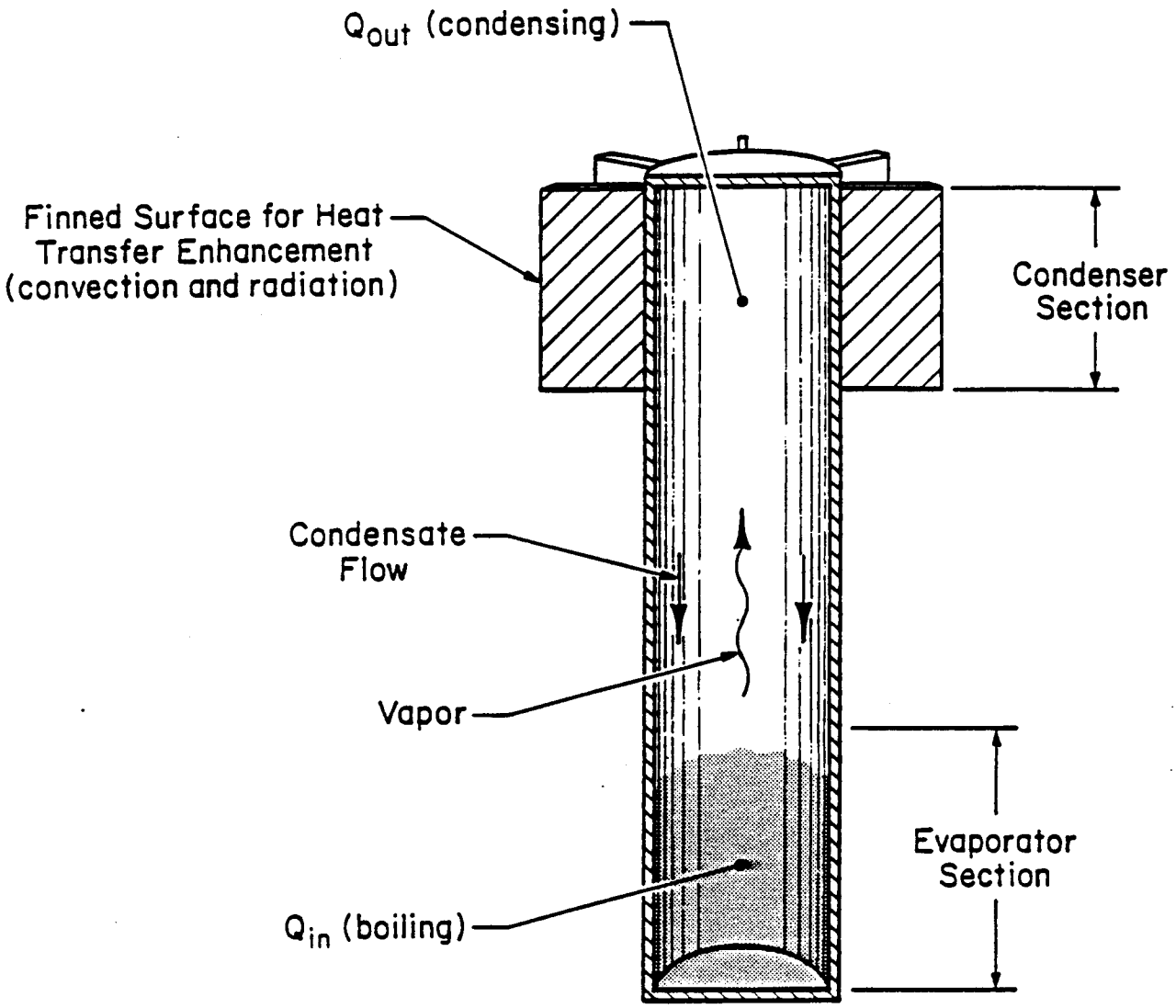

Figure 1. Heat transfer processes in a two-phase closed thermosyphon.

Haynes and Zarling (1982) and Zarling and Haynes (1984) did field testing of thermosyphons with inclined evaporators. Upon the completion of their last study it was realized that a similar investigation under controlled laboratory conditions was needed. The objective of this project was to determine performance of two standard, commercially available thermosyphons. The units tested were a CO_2 filled unit purchased for $1,900 from Arctic Foundations in Anchorage, Alaska, and a NH_3 filled unit purchased for $3,500 from Mobile Augers and Research Ltd., in Edmonton, Alberta, Canada. It took about 6 months to obtain the NH_3-filled unit because of the unavailability of the finned section.

This report first describes the history and applications of thermosyphons in cold regions. Then the operating characteristics are discussed including the selection of container, working fluid and finned surface. The performance of the finned surface is a major consideration in design because the largest portion of the total heat transfer resistance is due to this component. Next the test setup and the results are presented for thermosyphon performance with tilted evaporator sections. We present a design methodology that can help in sizing a thermosyphon installation.

HISTORY

The invention of the thermosyphon as a heat transfer device dates back to at least the 1800s. Perkins and Buck (1892) in a series of patents issued by the United Kingdom described single-phase and two-phase thermosyphons. His last patent covered a sealed tube partially filled with a liquid (he suggested liquids ranging from antifreezes to water to those of higher boiling points). In the United States, F.W. Gay (1929) patented the thermosyphon (Perkins Tube) with external fins for application in gas-to-gas heat exchangers.

A patent granted to Richard S. Gaugler (1944) and assigned to the General Motors Corporation covered both the thermosyphon and heat pipe. He described the devices as closed systems partially filled with a volatile liquid wherein heat is absorbed at one point by evaporation of the liquid and is dissipated at another point by the condensation of the

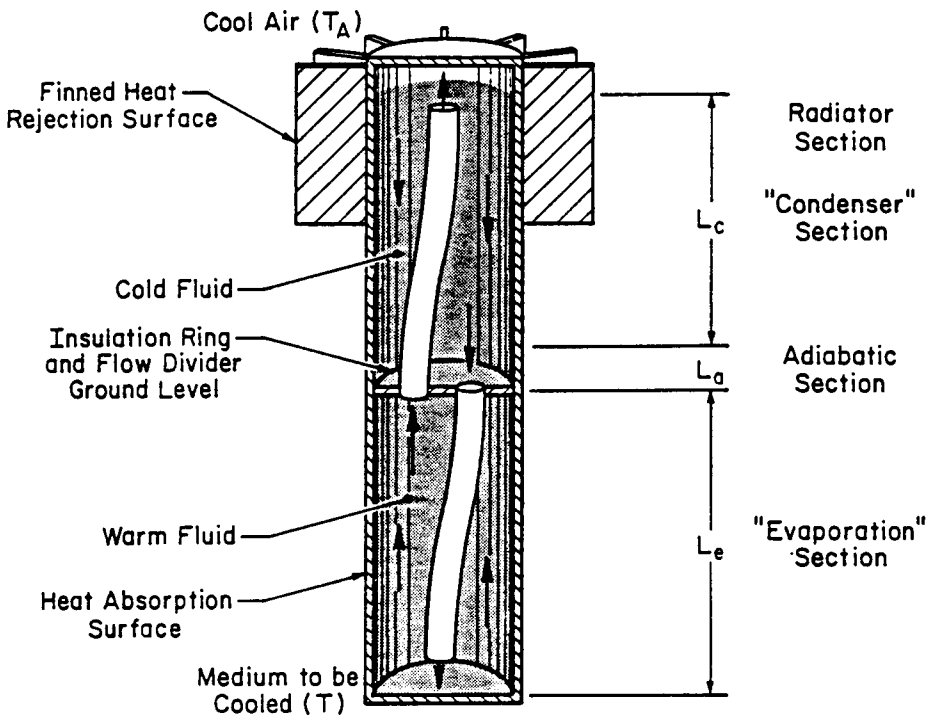

Figure 2. Balch single phase thermosyphon.

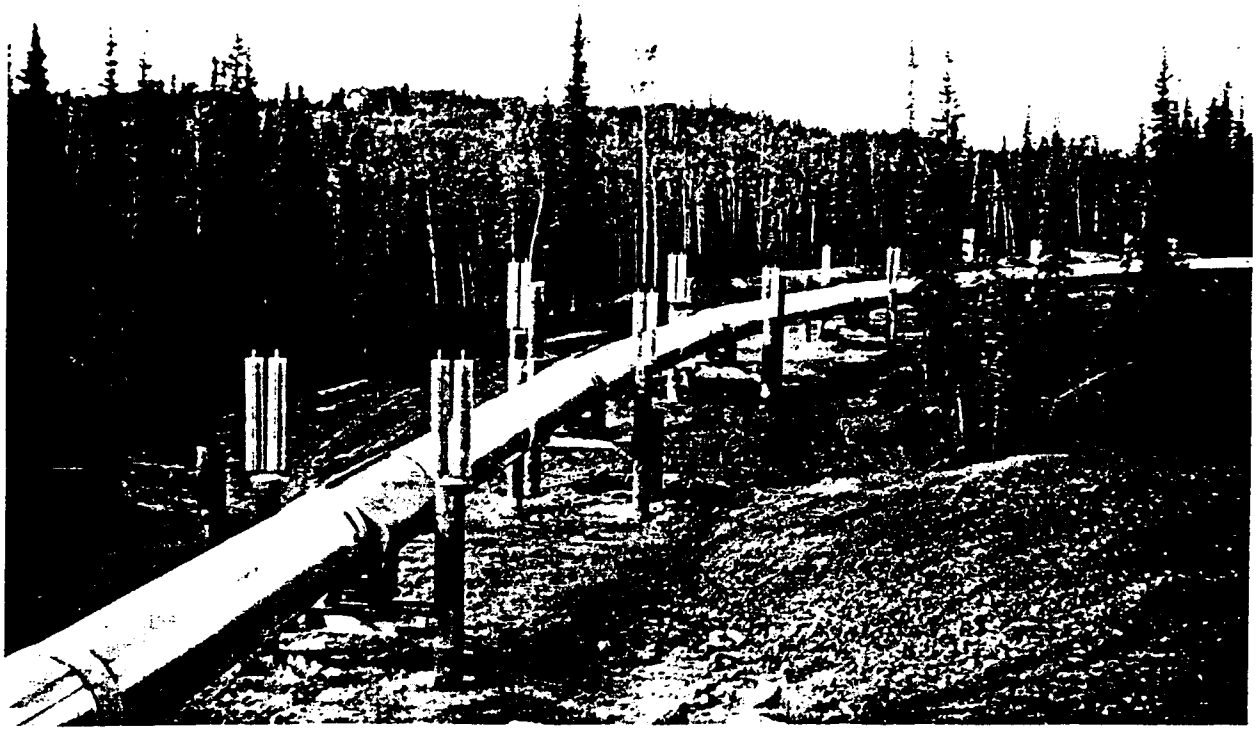

Figure 3. McDonnel Douglas "Cryoanchor" thermosyphons used on TAPS in Alaska.

generated by the thermal expansion (decrease in density) of the liquid in the below-ground section and thermal contraction (increase in density) of the liquid in the above-ground section. Thermal energy is transferred from the ground to the liquid flowing in the loop and then to the cold ambient air surrounding the finned section. The influence of loop configuration on closed loop thermosyphon performance was studied by Chen (1982).

Air convection piles have been analyzed and tested as permafrost protection devices using forced flow driven by a fan (Reed, 1966) and natural convection flow (open single-phase thermosyphon; Reid, 1974). Reid (1983) extended his work to examine the influence of frost formation on the heat exchange surfaces within the pile on thermal performance.

During construction of the Alyeska Trans-Alaska Pipeline, TAPS, more than 100,000 McDonnell Douglas (1974, 1978) Cyro-Anchors were installed in the vertical support members (piles) supporting the 400-mile, above-ground portion of the pipeline. It was this project that generally increased the engineer's awareness of the application of thermosyphons to foundation stabilization on permafrost. Numerous papers and reports have been presented and published covering the design, operation and installation of the two-phase, ammonia-charged thermosyphons used on this project. Application papers include those by Jahns et al. (1973), Waters (1973), Waters et al. (1975), Galate (1976), Pearson (1977) and Heuer (1979). The following excerpt is taken from Heuer describing the thermosyphons used on the TAPS project.

> "The thermosyphons used on the pipeline were designed to transfer a minimum of 12 watts/ft of below ground embedment for a 3°F temperature difference between the evaporator and condenser sections. To ensure good heat transfer at higher temperature differences, a second performance criterion of 18 watts/ft for a 6°F temperature difference was also included in design. The heat pipes (thermosyphons) are made of mild carbon steel, and ammonia is the working fluid. The inner diameter is 1.5 in and the outer diameter is 2.0 in. The wall thickness was determined by requirements for handling during

manufacturing, transportation, and installation and external corrosion resistance rather than pressure vessel requirements. The lengths range from 28 ft to 75 ft. The ammonia charge varies with length. It includes the amount of ammonia in the liquid film and the gas phase when the thermosyphon is operating at design conditions plus a residual liquid pool which serves as a safety margin. Typically, when the heat pipe is inactive, the liquid pool at the bottom of the heat pipe is 1 to 2 ft deep.

A uniform circumferential distribution of the liquid film along the evaporator section of the thermosyphon is necessary for good heat transfer. If the liquid is concentrated in one or two rivulets as it flows down the thermosyphon and only part of the evaporator surface is wetted, the overall thermal resistance of the thermosyphon can be significantly increased. To prevent this, the evaporator wall is artificially roughened to ensure an even fluid distribution.

To improve heat transfer between the heat pipe and the atmosphere, an extruded aluminum radiator is press-fit onto the upper portion of the thermosyphon. The press-fit provides a low contact resistance between the thermosyphon and radiator. The radiator has 20 vertical fins with an outer diameter of 10.9 in. The fin surface areas is 12.6 ft^2/ft of radiator length. For thermosyphon lengths of 37 ft or less, the radiator length is 4 feet. For longer thermosyphons, a 6-foot radiator is used. Where the radiator is attached, the thermosyphon outer diameter is increased to 3 in. This provides the necessary stiffness for the pressing operation and mechanical protection after the thermosyphons are installed."

Presently, two firms are fabricating two-phase thermosyphon devices for northern applications: Arctic Foundations owned by Erwin Long of Anchorage, Alaska, and Mobile Augers and Research Ltd., Edmonton, Alberta. The second firm is licensed to produce the McDonnell Douglas "Cyro-Anchor."

In addition to the pipeline use as shown in Figure 3, other applications of the two-phase thermosyphon include slab-on-grade building foundations (Figure 4; after Hayley, 1982); roadways (Figure 5); railroad beds (Figure 6; after Hayley et al., 1983); transmitter towers (Figure 7; after Long and Yarmack, 1982); landing fields (Figure 8); and building piles (Figure 9; after Long and Yarmack, 1982). One other northern application is the use of thermosyphons to prevent roadway icing on bridge decks (Ferrara and Brinkman, 1976). Thermosyphons have been made from soft copper tubing to wrap around a pile and from steel tubing to be inserted in or alongside of the pile. In some cases, the pile itself has been used as the sealed container. Radiator portions (heat rejection or condenser) of the tubes have ranged from bare pipe, to segmented radial fins, to longitudinal fins. Fin materials have been either steel or aluminum.

The remainder of this report will examine the heat transfer design aspects of a thermosyphon. Because the two-phase thermosyphon has the largest potential for arctic applications, attention will only be focused on this type of device. To advance foundation design using the two-phase thermosyphon, a thorough knowledge of the operating characteristics of these devices is desirable.

WORKING FLUID

The choice of a working fluid for a thermosyphon is based on several parameters. The working fluid must have an adequate vapor pressure at low operating temperatures, high operating thermal conductivity, a freezing point compatible with low temperature operation, and high density and low viscosity to enhance flow return and turbulence. The working fluid must be chemically stable and compatible with the container material. In arctic applications, propane, butane, carbon dioxide, Freons and ammonia have been used as working fluids.

It is important that the thermosyphon operate during periods of extremely low temperatures. To accomplish this, the vapor pressure of the working fluid must be high to transport sufficient mass in the vapor phase for adequate heat transfer. Saturation vapor pressure as a

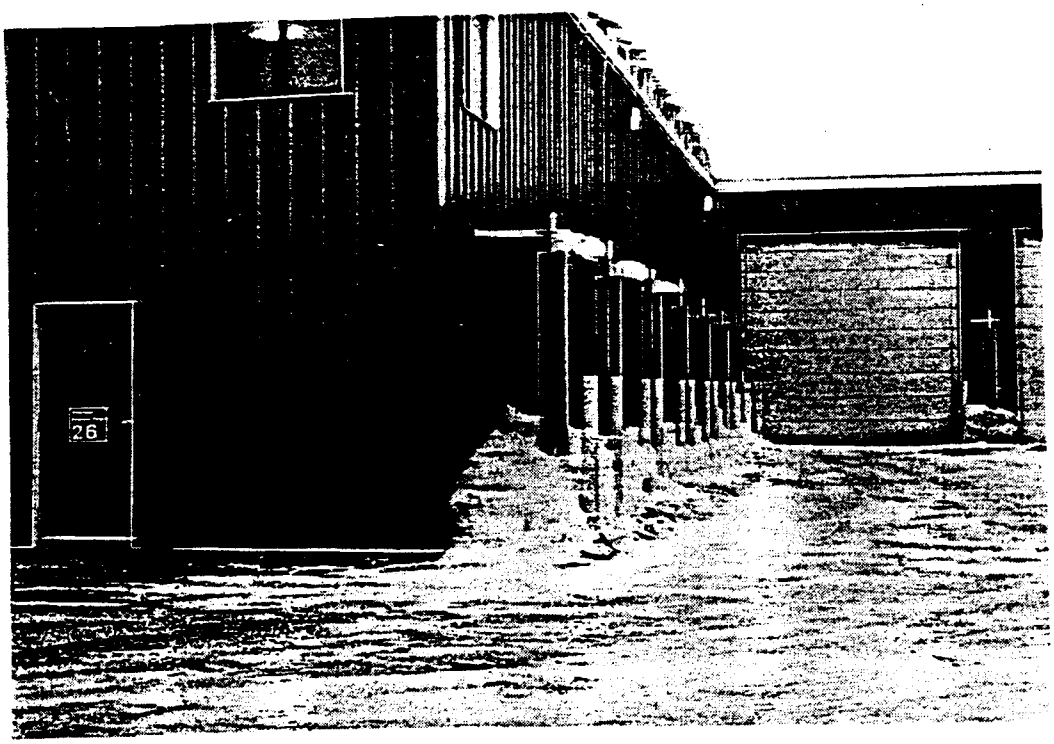

Figure 4. Thermosyphons used to remove heat below a slab-on-grade foundation on permafrost, Prudhoe Bay, Alaska.

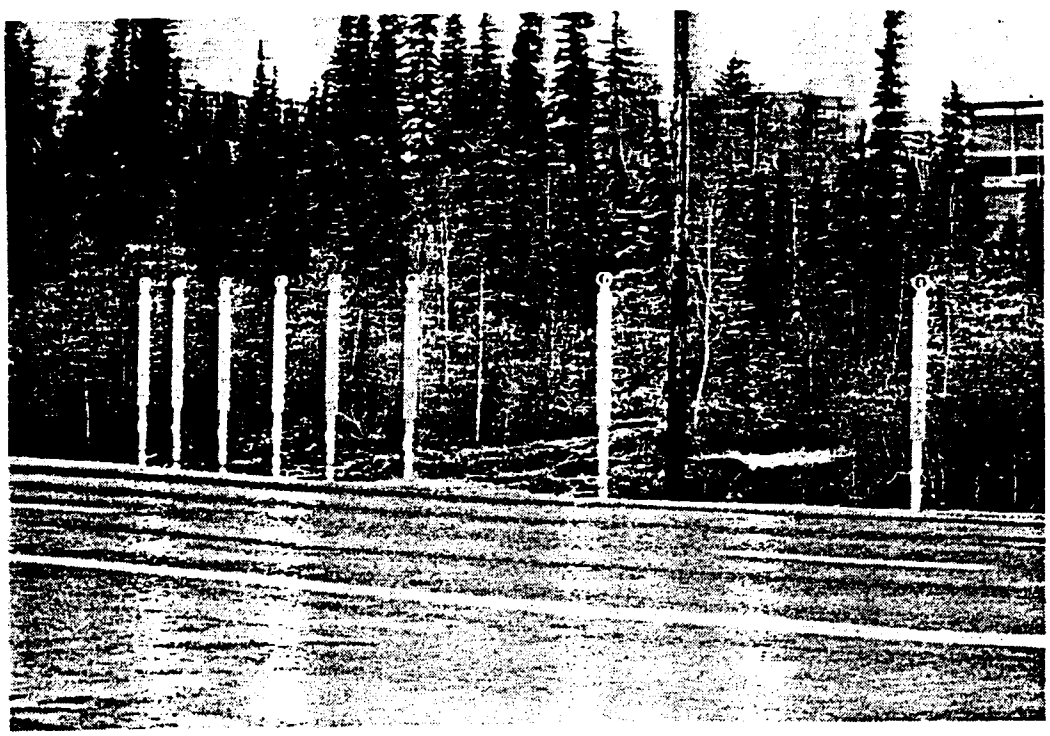

Figure 5. Thermosyphons installed below a roadway crossing ice-rich ground, Fairbanks, Alaska.

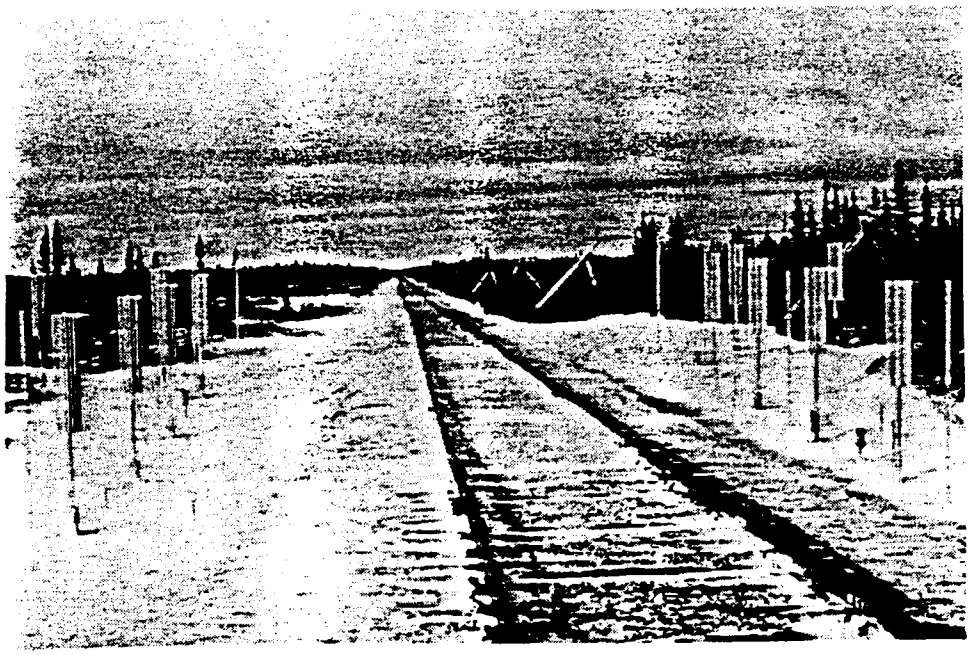

Figure 6. Thermosyphons used to stabilize a railroad bed crossing ice-rich ground (photo by Don Hayley).

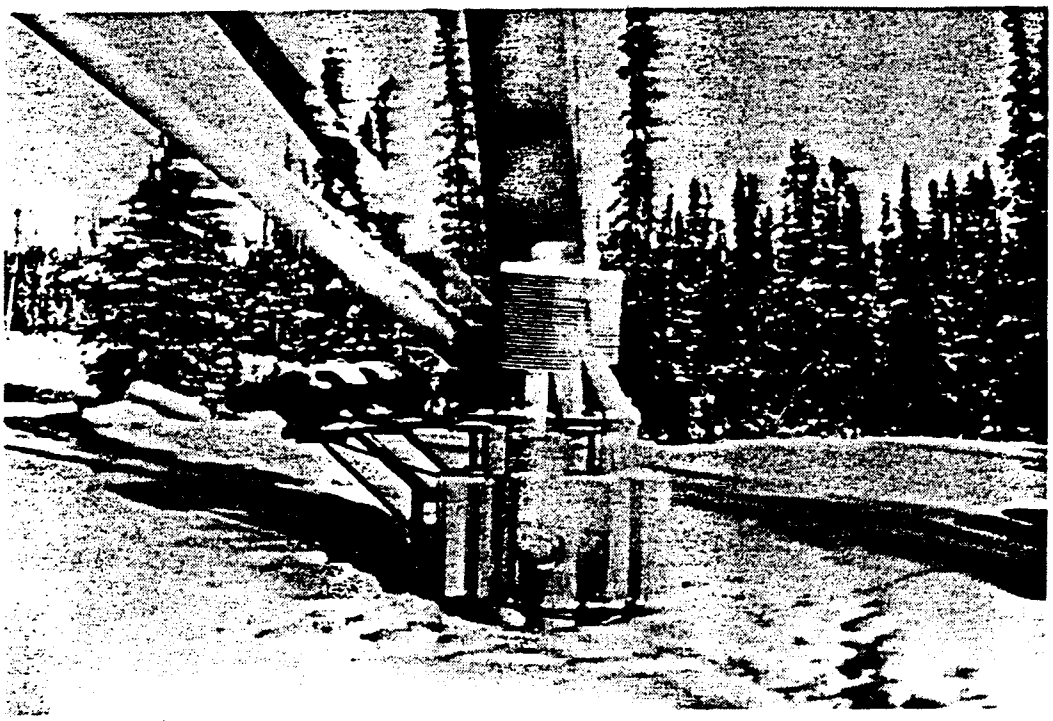

Figure 7. Thermosyphons used to stabilize permafrost below foundation on a transmitter tower (photo by Erv Long).

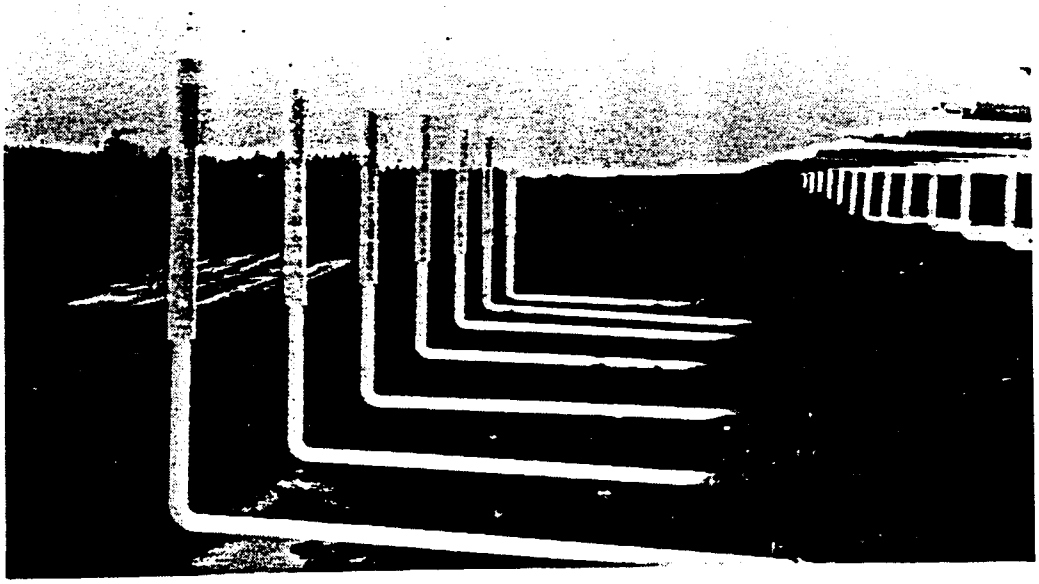

Figure 8. Thermosyphons installed below a section of paved runway of Bethel airport, Alaska (photo by Erv Long).

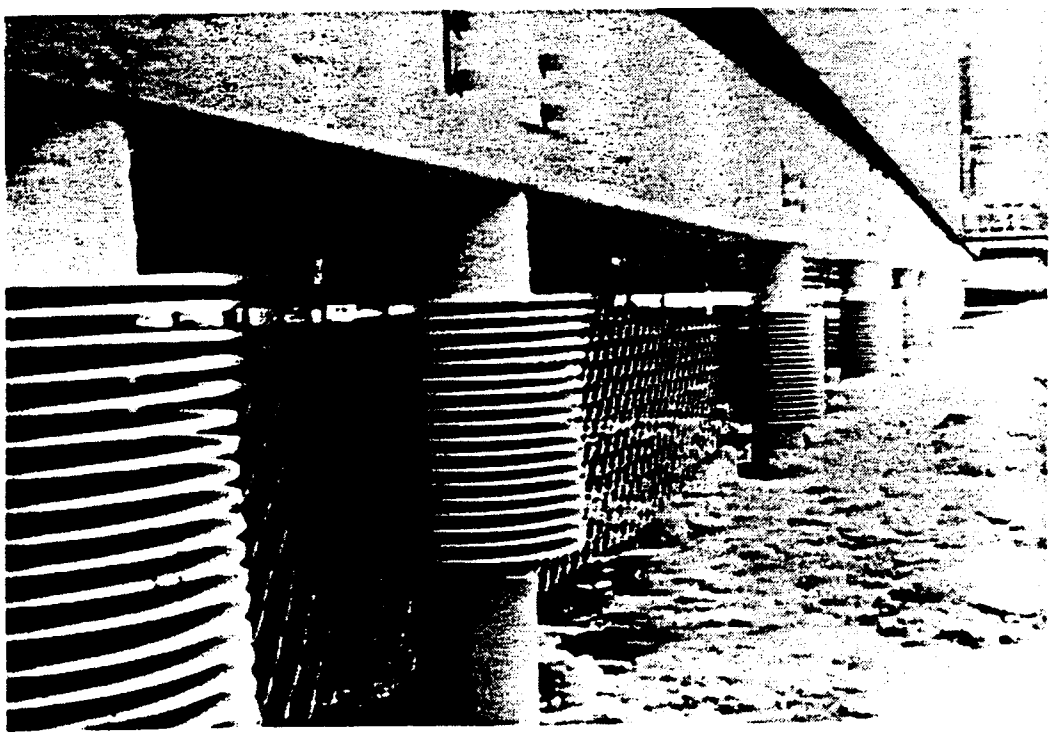

Figure 9. Thermosyphons incorporated into building pile foundations in permafrost area (photo by Erv Long).

function of saturation temperature is shown in Figure 10 for several working fluids (ASHRAE, 1981). A question often asked is: "What is the pressure of the working fluid in a thermosyphon?" Figure 10 shows that saturation vapor pressure and temperature are not independent thermodynamic properties. Once the temperature is fixed for a pure fluid, the vapor pressure is also fixed. Changing the liquid temperature in the evaporator changes the vapor pressure so that thermodynamic equilibrium is reachieved at saturation conditions.

The chemical compatibility of the working fluid and the thermosyphon tube material is a concern as it relates to the potential for generation of noncondensable gases within the tube. The formation of noncondensable gases results in the blockage of the working fluid vapor from reaching the entire length of the condenser with a subsequent reduction in thermal performance. Particular attention must be directed toward proper cleaning of the thermosyphon tube prior to filling to ensure compatibility and suitability of cleaning agents with the working fluid and tube material. Any chemical instability due to the cleaning process or cleaning agents may lead to the formation of noncondensable gases. Blockage may also occur from incomplete evacuation of units prior to charging. The degree of blockage from noncondensable gases is directly proportional to operating temperature and inversely proportional to operating pressure. The higher the pressure, the smaller the volume occupied by a given mass of gas. Compatibility of several thermosyphon fluids with tube materials is given in Table 1. The physical properties of several working fluids are given in Table 2 (ASHRAE, 1981).

Accumulation of noncondensable gases in the thermosyphon result in cold topping. Under field conditions, infrared temperature monitors or surface thermometers are typically used to detect the formation of noncondensable gases. Caution must be exercised, however, in interpreting the results of thermal surveys of this nature. For example, a properly working thermosyphon will likely "shut-off" if warm weather occurs shortly after an extreme cold spell. This condition will continue until the ground temperature rises above air temperature and the thermosyphon becomes operational again. During this "shut-off" period, the radiator portion of the thermosyphon will appear cold.

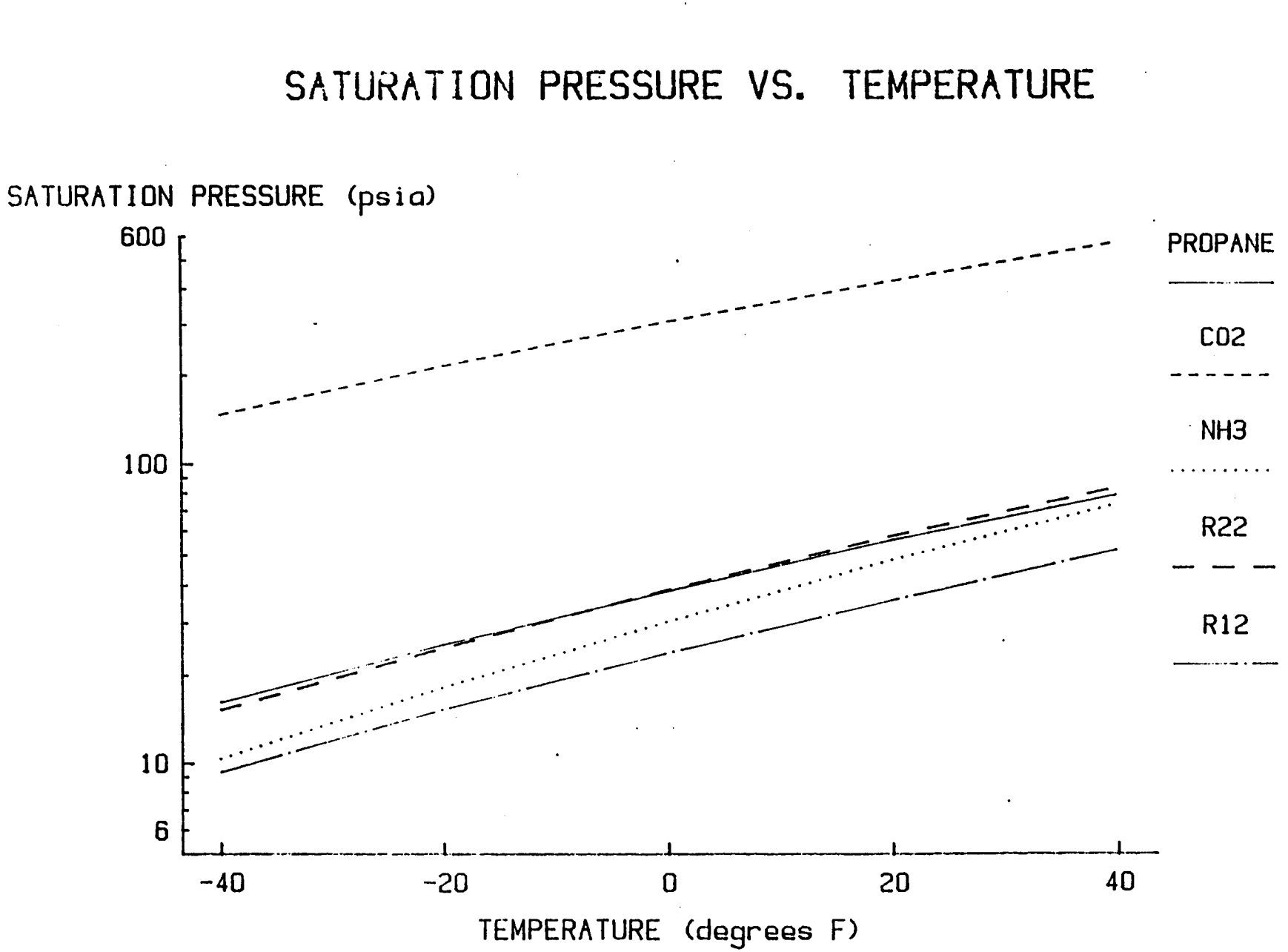

Figure 10. Saturation vapor pressure as a function of saturation temperature.

TABLE 1. Toxicity, flammability and metal compatibility of several working fluids where H = highly, M = mildly, S = slightly, C = compatible, N = non (adapted from ASHRAE, 1981; Basiulis and Prager, 1975).

Fluid	Toxic	Flammable	Steel	Aluminum	Copper	Stainless
Ammonia	H	S	C	C	N	C
Freon-22	M	N	C	C	C	C
Carbon-dioxide	M	N	C	C	C	C
Propane	S	H		C		
Butane	S	H		C		

CONTAINER

Containers for thermosyphons have been fabricated of mild steel, aluminum, copper and in special applications stainless steel. Even though most units are used in areas of very low temperature, the heating of the condensers by the working fluid during cold weather raises the tube wall temperature, reducing the potential of low-temperature brittle failure of the steel tube.

Container materials must also be compatible with the charging fluid (Table 1), fluid pressures and structural loads as required by design. The highest pressure working fluid used to date is CO_2 with a pressure of over 500 psi at 32°F. This is well below the allowable pressure for Schedule 40 steel piping for most diameters of thermosyphons manufactured.

Materials used for heat dissipation fins must be thermally conductive and resistive to corrosion. Although materials with the highest possible thermal conductivity appear most favorable, desired fin conductance can also be achieved by using thicker fins made of materials

TABLE 2. Thermal-physical properties of working fluids at 0°F and 20°F (ASHRAE, 1981).

Property	Carbon dioxide CO_2		Ammonia NH_3		Propane		Freon 22 R22		Freon 12 R12	
	0°F	20°F	0°F	20°F	0°F	20°F	0°F	20°F	0°F	20°F
Viscosity, liq. lbm/ft-hr	0.291	0.252	0.552	0.488	0.381	0.344	0.646	0.592	0.767	0.687
Viscosity, vap. lbm/ft-hr	0.327	0.350	0.0234	0.0243	---	---	0.0266	0.0279	0.0265	0.0279
Thermal Cond., liq. Btu/hr-ft-°F	0.077	0.069	0.335	0.321	0.068	0.065	0.063	0.060	0.0490	0.0467
Specific heat, liq. Btu/lbm-°F	0.486	0.543	1.083	1.092	0.562	0.577	0.271	0.276	0.217	0.220
Specific heat, vap. Btu/lbm-°F	0.309	0.346	0.590	0.620	0.403	0.425	0.158	0.165	0.145	0.150
Heat Vaporization Btu/lbm	120	118	569	568	169	163	100	91	69	66
Density, liq. lbm/ft^3	63.5	63.0	41.3	41.3	34.5	33.7	83.8	81.6	90.6	88.5
Specific vol., vap. ft^3/lbm	0.291	0.271	9.12	8.91	2.68	1.88	1.37	0.94	1.61	1.10
Prandtl Number, liq.	1.67	1.98	1.78	1.66	3.15	3.05	1.53	2.27	3.4	3.2
Surface tension $lbf/ftx10^3$	0.63(13°F) 0.08(68°F)		1.61(52°F)				0.55(80°F)		---	---

with lower thermal conductivity. Common fin materials are aluminum and mild steel.

Special surface treatments are used to inhibit corrosion, alter the appearance, increase infrared emmissivity, decrease solar absorptivity, and alter soil-container adfreeze bond strength. Aluminum may be anodized to reduce corrosion and to improve emmissivity. Steel is normally coated with a paint to minimize or eliminate corrosion and at the same time provide high infrared emmissivity and low solar absorptivity. Table 3 gives infrared emmissivity, ε, and solar absorptivity, α_s, data for some commonly used coatings.

TABLE 3. Infrared emmissivity and solar absorptivity of selected surfaces (ASHRAE, 1981).

Surface	ε	α_s
Anodized aluminum	0.82	0.14
White acrylic paint	0.90	0.26
White zinc oxide paint	0.92	0.16
White aluminum oxide	0.98	0.84
Black parsons paint	0.98	0.98

Thermosyphon Conductance

In this study, the overall heat transfer conductance of the closed two-phase thermosyphon is defined as

$$C = Q/(T_s - T_a) \qquad (1)$$

where T_a is the ambient air temperature, and T_s is the temperature of the evaporator on the outside surface of the pipe. The overall conductance, C, will be used throughout the remainder of this report when referring to the overall performance of the thermosyphon device.

The reciprocal of the overall conductance is thermal resistance. It includes the convective and radiative resistances of the heat-dissipating fins, the fin resistance, the pipe wall resistance, and the condensation and evaporation resistances which are shown schematically in Figure 11. In equation form, the reciprocal of the overall conductance is

$$1/C = 1/KL_c\pi D + \ln(D'/D)[1/L_c + 1/L_e]/2\pi k_p + 1/C' \qquad (2)$$

where L_c and L_e are the lengths of the condenser and evaporator, K is the total air-side conductance, D' and D are the outside and inside diameters of the pipe, and k_p is the thermal conductivity of the pipe. Typical values for the overall conductance for ammonia-filled and CO_2-filled devices range from 5 to 20 Btu/hr-F°. The last term in equation 2 defines the thermosyphon conductance, C', which only depends on the evaporation and condensing heat transfer coefficients. This conductance is defined as

$$C' = \left(\frac{1}{1/\pi Dh_c L_c + 1/\pi Dh_e L_e}\right) \qquad (3)$$

where h_c and h_e are the condensing and evaporating heat transfer coefficients. Using this definition, the heat transfer rate for the thermosyphon becomes

$$Q = C'(T_e - T_c) \qquad (4)$$

where T_e is the inside wall temperature at the evaporating section and T_c is the inside wall temperature at the condensing section.

Applying a dimensional analysis to a thermosyphon, it can be shown that the heat transfer conductance depends upon the fill ratio, V^+, ratio of liquid volume to total tube volume, ratio of heated to cooled length, L^+, ratio of heated length to tube diameter, liquid saturation temperature, T_{sat}, heat flux, type working fluid and angle of inclination. Lee and Mital (1972) have investigated all but the angle of inclination effect.

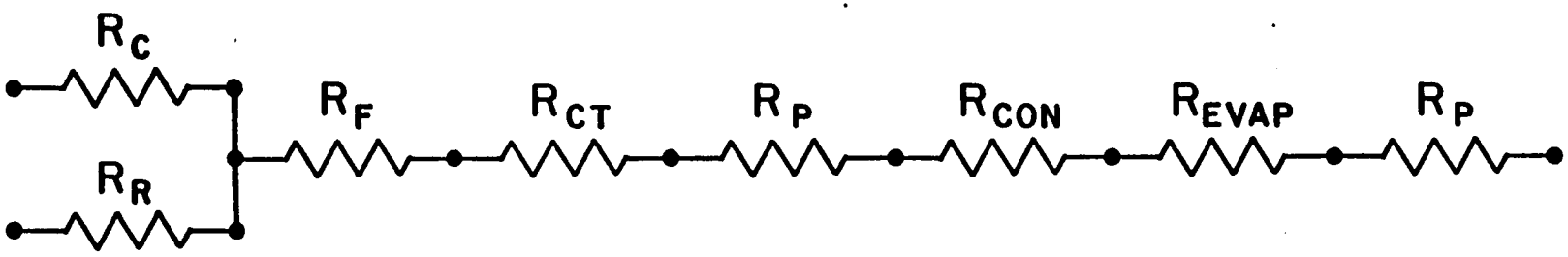

Figure 11. Schematic of electrical analog circuit modeling thermosyphon device where

R_c = convective air-side resistance
R_r = radiative air-side resistance
R_f = fin resistance
R_{ct} = contact resistance
R_p = pipe wall resistance
R_{con} = film condensation resistance
R_{evap} = evaporation or boiling resistance

Their results were based on both an experimental and analytical analysis of the thermosyphon. They found the maximum heat flux and heat transfer conductance increased with fill ratio up to a certain quantity and then became independent of V^+. The maximum heat transfer conductance increased with a decrease in the heated-to-cooled length ratio, L^+. An increased condenser length will increase thermosyphon performance if this result is valid. The heat transfer conductance increases with increasing pressure inside the thermosyphon. This is expected as the boiling heat transfer coefficient increases as the saturation vapor pressure of the working fluid increases. The density of the vapor also increases with increasing saturation pressure, resulting in a lower vapor velocity and a smaller interfacial shear on the falling liquid film. The heat transfer conductance increased with increasing heat flux, although this effect decreased with increasing operating pressure. The type of working fluid has a significant effect on the heat transfer conductivity. Generally speaking, a liquid with a high thermal conductivity, high latent heat, high vapor density and low viscosity at saturation will yield higher heat transfer conductances. However, these are not the only criteria that should be used in choosing the working fluid. Other considerations such as cost, toxicity, compatibility with thermosyphon tube materials and saturation pressure at operating temperatures are also important.

In a later study, Clements and Lee (1981) concluded that the overall heat transfer coefficient is strongly affected by the tube diameter. A decrease in the overall conductance occurs with increasing tube diameter brought about mainly by changes in the evaporative and convective resistances. The convective resistance in their study occurred on the outside of a bare tube. Wall thickness and an L/D ratio in range of 5 to 30 have little effect on performance.

HEAT TRANSFER FROM THE FINNED SECTION

Two types of fins have been commonly used on thermosyphons: the straight fin of rectangular cross section, Figure 12, and the annular fin of rectangular cross section, Figure 13. Fins can be extruded or

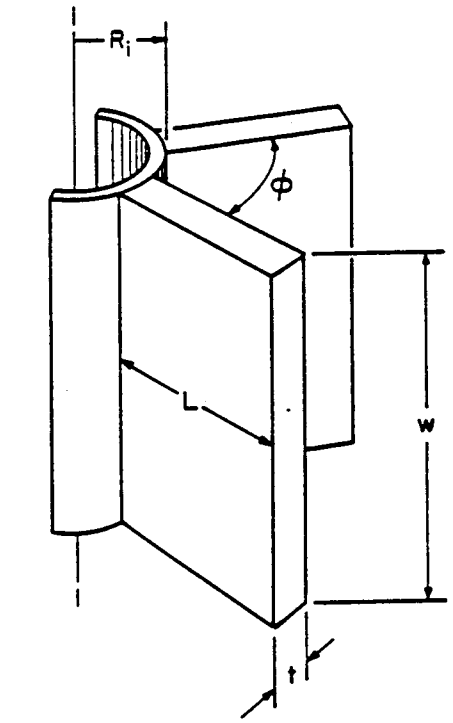

$$P = 2w + 2t$$

$$A_c = wt$$

$$A_f = wt + (2w+2t)L$$

$$m^2 = hP/KA_c$$

Figure 12. Rectangular fin of uniform cross section.

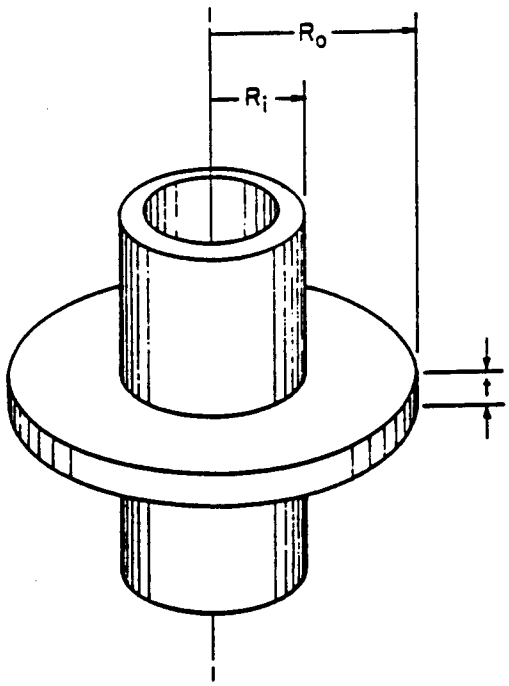

$$\alpha = R_i/R_o$$

$$\beta^2 = 2hR_o^2/Kt$$

Figure 13. Annular fin of uniform thickness.

broached from a thick-walled tube, stamped from sheet metal and installed on the tube, or tension wrapped on the base tube in a helix fashion. For the later method, mechanical bonds are often just the tension winding of the fins. For low-temperature applications, epoxy resins are sometimes used to bond fins and improve thermal contact. If thermal expansion and/or contact resistance are important, then brazing or welding of the fins to the tube is preferred.

The air-side heat transfer coefficient on the finned section of a thermosyphon is typically 10 to 50 times smaller than the boiling and condensing coefficients on the tube side. The use of a finned surface will increase the air-side conductance (hA) by greatly increasing the heat transfer surface area. The use of an extended surface provides greater balance in the thermal resistances on each side of the tube resulting in an improved thermal design. The parameters effecting air-side conductance are:

1. fin spacing;
2. fin efficiency; and
3. special fin configurations to increase the heat transfer coefficient.

The significance of each of these factors can be evaluated by defining the overall heat transfer coefficient, U_i, based on the internal tube area as

$$U_i = \left(\frac{1}{A_i/\eta hA + 1/h_i}\right) \tag{5}$$

The total surface efficiency, η, in equation 5 is defined as

$$\eta = 1 - (1-\eta_f)\frac{A_f}{A} \tag{6}$$

where

A_f = fin surface area
η_f = fin efficiency

A_i = inside surface area of tube
η = total surface efficiency
A = total air-side surface area including area between fins
h = air-side heat transfer coefficient ($h_c + h_r$)
h_i = tube-side heat transfer coefficient

The air-side conductance, K, can be defined as

$$K = \eta\, hA/A_i \tag{7}$$

so equation 5 becomes

$$U_i = \left(\frac{1}{1/K + 1/h_i}\right) \tag{8}$$

An increase in fin pitch (number of fins per unit length) will increase the air-side conductance by increasing the ratio of A/A_i. However, very small fin spacing (increased fin pitch) will increase the cost of the finned tubing and can lead to a reduction in the air-side heat transfer coefficient due to boundary layer interference.

Increasing the total surface efficiency will also increase the air-side conductance. Fin efficiency and, therefore, surface efficiency are influenced by the fin thickness, length and thermal conductivity. Fin efficiency is defined as the ratio of the actual heat transfer taking place from the fin to the heat transfer that would take place if the entire fin surface were at its base temperature. Therefore,

$$\eta_f = Q_{act}/Q_{max} = Q_{act}/hA_f(T_b - T_a) \tag{9}$$

where

T_b = base temperature of the fin
T_a = ambient air temperature.

Fin efficiency can be determined from either equations or charts given in the most basic heat transfer texts. For a rectangular fin of uniform cross section (Figure 12) the fin efficiency is given as

$$\eta_f = \frac{hPkA_f}{hA_f} \frac{\sinh mL + (h/mk)\cosh mL}{\cosh mL + (h/mk)\sinh mL} \qquad (10)$$

and for an annular fin of uniform rectangular cross section (Figure 13) the fin efficiency (Chapman, 1974) is given as

$$\eta_f = \frac{2\alpha}{\beta(1-\alpha^2)} \cdot \frac{K_1(\alpha\beta)I_1(\beta) - I_1(\alpha\beta)K_1(\beta)}{K_0(\beta)I_1(\alpha\beta) + I_0(\beta)K_1(\alpha\beta)} = G(\alpha,\beta) \qquad (11)$$

where α and β are nondimensional geometric and heat transfer parameters defined in Figure 13, I_0, I_1 and K_0, K_1 are the modified Bessell functions of the first and second kind and of zero and first order. Fin efficiency, $G(\alpha, \beta)$, is presented in Figure 14.

Analysis of conduction heat transfer in a fin shows that the maximum heat transfer per unit of fin material volume is obtained if a linear temperature gradient exists in the fin. To satisfy this condition, the fin cross-sectional area must decrease with distance from the fin base. Annular fins of uniform cross section do not satisfy this criterion. In fact, the amount of fin material increases with distance from the fin base. The use of segmented annular fins with constant cross-sectional area for heat conduction (Figure 15) offer an improvement over solid annular fins in approaching a linear temperature gradient. Another advantage of the segmented fin is a larger convective heat transfer coefficient due to interrupting development of the boundary layer as the flow separates from each fin. This effect is partially mitigated by the reduced surface area for heat transfer.

Fin spacing depends on the amount of extended surface area required to increase the air-side conductance to an economic level relative to the tube-side conductance. However, as the fin spacing is decreased, a point is reached where the boundary layers on adjacent fins will interfere, resulting in an increased air-side resistance. Furthermore, the heat transfer benefits decrease for values of K greater than h_c. The convective heat transfer parameter or Nusselt number correlations,

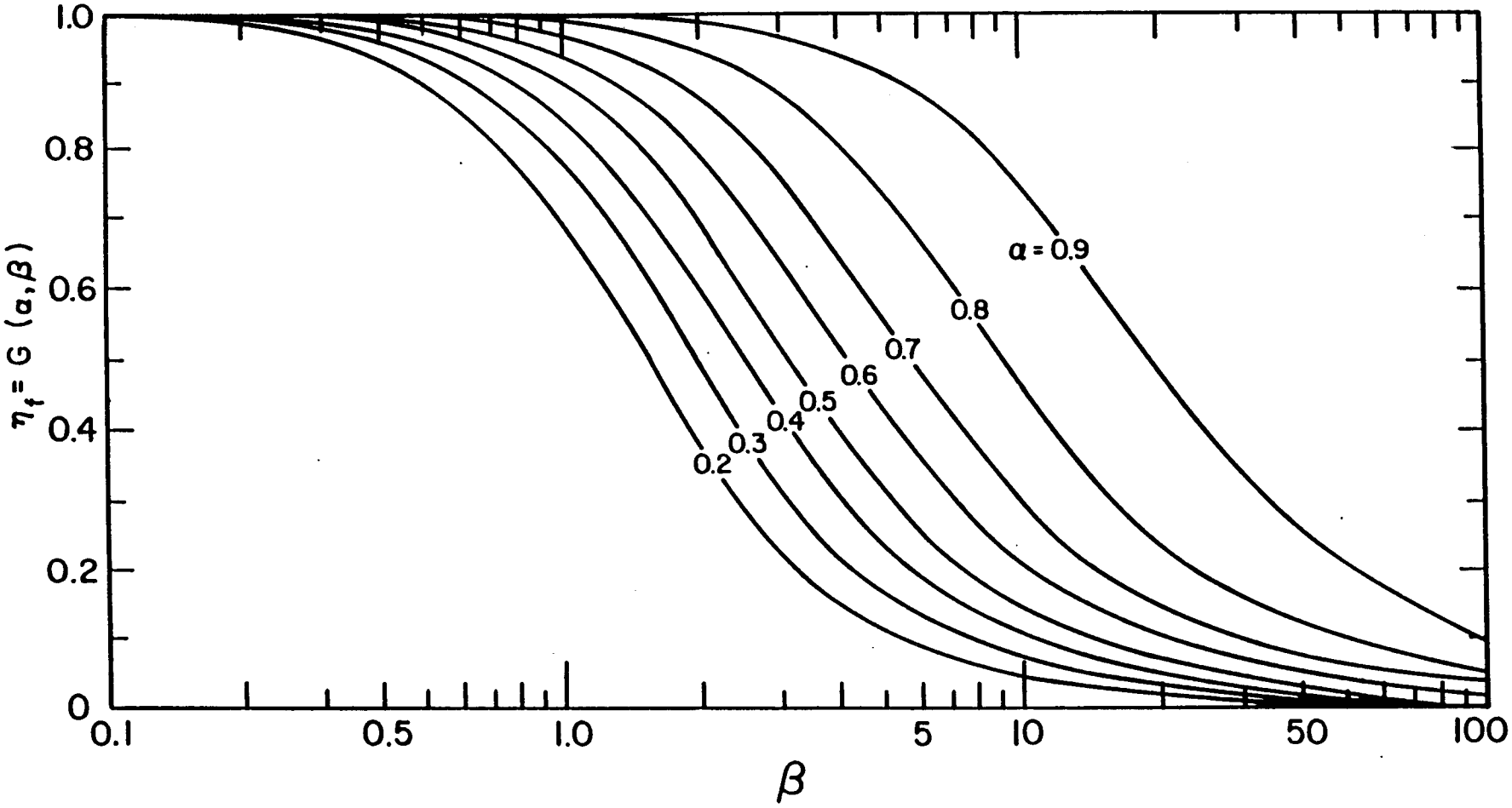

Figure 14. The funtion G for an annular fin of uniform thickness.

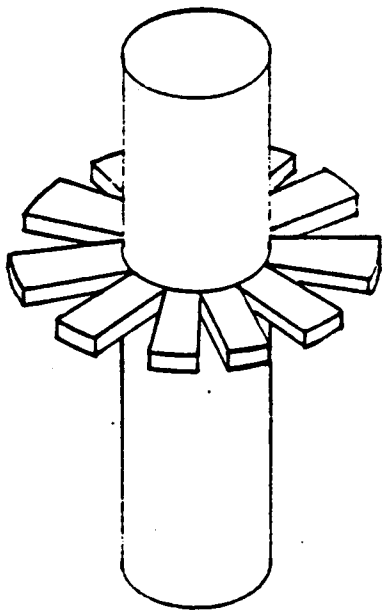

Figure 15. Segmented annular finned tube.

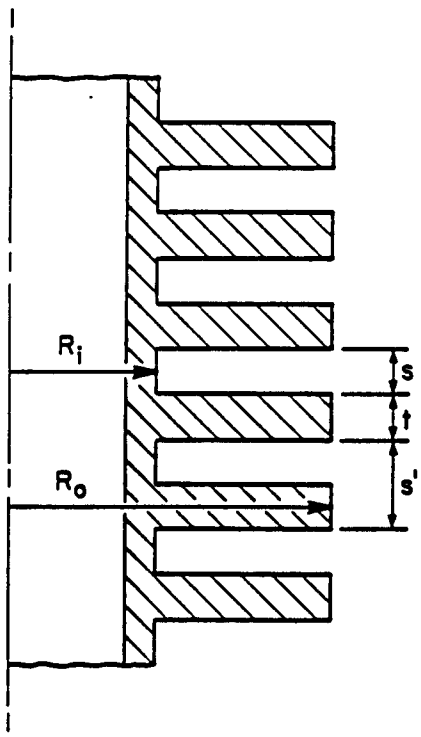

Figure 16. Annular fin cross section.

Nu = hD/k, have been developed by Briggs and Young (1963) for annular finned tubes in a six-row tube bank under forced convection conditions. Their equation shows that increasing fin spacing (reducing fin pitch) increases the Nusselt number as anticipated. Doubling the fin spacing leads to a 21% increase in the forced convective heat transfer coefficient but reduces the fin surface area per unit length by 50%, yielding a 40% reduction in the total surface conductance.

For longitudinal rectangular fins on a circular tube, no known correlations exist for predicting the convective heat transfer coefficient for the finned surface in cross flow.

In natural convection, fins generally need a high fin efficiency (80 to 90%) for optimum heat transfer. A low fin efficiency reduces the tip ΔT, the difference between fin tip and ambient air temperatures, thus decreasing the convective heat transfer coefficient. As in forced convection, the free convection heat transfer coefficient decreases as the number of fins increases beyond a given fin pitch. This is due to the interference of convection currents on adjacent fins caused by the reduction in flow passage area. No known heat transfer correlations exist for horizontal annular fins or vertical longitudinal rectangular fins attached to a vertical circular tube in free convection. However, there are a few predictive relationships given in the literature for vertical parallel fins.

Heat transfer from the finned surface of a thermosyphon also includes the radiation mode. Under windy conditions, the dominant mode of heat transfer is convection, and the radiation losses can be neglected. However, at very low wind speeds, the radiation mode can become significant. In fact, it can approach the convective heat transfer rate in magnitude. Because the convective and radiation modes of heat transfer act in parallel, the conductances for each mode can be added together to yield a total surface conductance. The total surface conductance would then be substituted into equation 7 to calculate the finned surface conductance, K.

For longitudinal rectangular finned thermosyphons, the radiation heat transfer coefficient for isothermal surface conditions is

$$h_r = \frac{\sigma\varepsilon(T_s^2 + T_\infty^2)(T_s + T_\infty)}{1 + \varepsilon(\xi-1)} \qquad (12)$$

For isothermal annular finned thermosyphons, the radiation heat transfer coefficient can be derived from Sparrow et al. (1962) as

$$h_r = \sigma\varepsilon(T_s^2 + T_\infty^2)(T_s + T_\infty)(1-F)\left(\frac{1}{\frac{R}{H} - \frac{1}{RH} + \frac{1}{R}}\right) \qquad (13)$$

or

$$h_r = \sigma\varepsilon(T_s^2 + T_\infty^2)(T_s + T_\infty)B$$

where

$$B = (1-F)(1/[1/R-1/RH+R/H]$$

$$F = 1 - \frac{1}{R} + \frac{1}{\pi}\left(\frac{2}{R}\tan^{-1}\left\{\frac{2(R^2-1)^{1/2}}{H}\right\}\right.$$

$$- \frac{H}{2R}\left\{\frac{(4R^2 + H^2)^{1/2}}{H}\sin^{-1}\left[\frac{4(R^2-1) + \frac{H^2}{R^2}(R^2-2)}{H^2 + 4(R^2-1)}\right] - \sin^{-1}\left(\frac{R^2-2}{R^2}\right)\right.$$

$$\left.\left. + \frac{\pi}{2}\left[\frac{(4R^2 + H^2)^{1/2}}{H} - 1\right]\right\}\right)$$

$R = R_o/R_i$

$H = S/R_i$

T_s = mean surface temperature of fin

T_∞ = radiant temperature of surroundings

σ = Stefan-Boltzmann Constant

ε = surface emmissivity

$\xi = (2L+R_i\phi)/2(L+R_i)\sin(\phi/2)$

The geometric variables use in these definitions are shown in Figures 12, 13 and 16. A plot of the view factor "F" is shown in Figure 17 for annular fins. The interpretation of this graph is that as the fin spacing, S, decreases or the radius ratio, R, increases, the

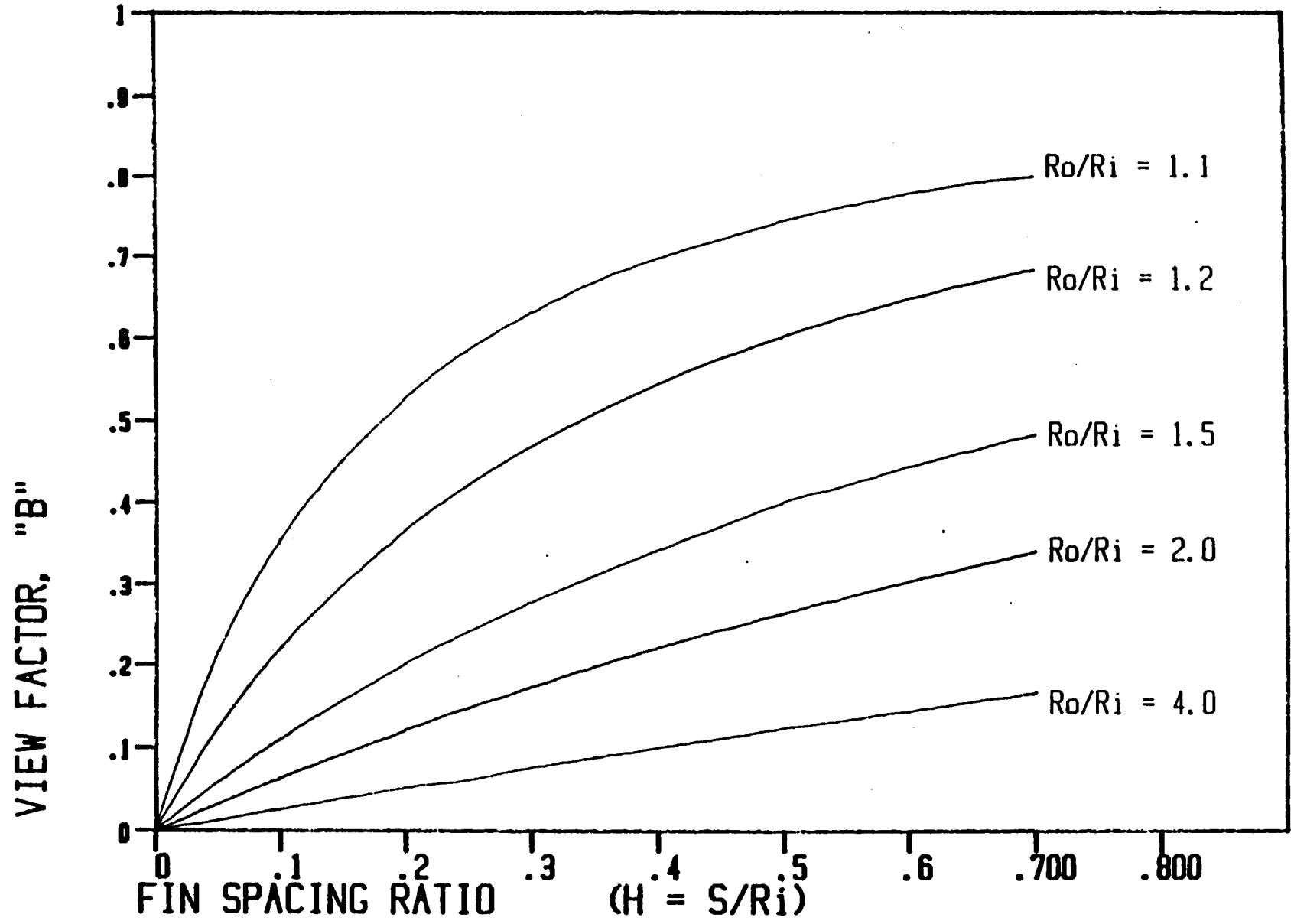

Figure 17. Annular fin view factor.

effectiveness of the finned surface to radiate energy to the surroundings is decreased.

The radiant temperature of the surroundings can be conservatively assumed as the ambient air temperature. Under clear sky conditions, the radiant sky temperature will be colder than the ambient air temperature. Swinbank (1963) presented a simple relationship for calculating the effective sky temperature under conditions of zero cloud cover.

$$T_{sky} = 0.0412\ T_{air}^{1.5} \tag{14}$$

where T_{sky} and T_{air} are both degrees Rankine. Another popular equation for calculting sky temperature comes from Bliss (1961)

$$T_{sky} = T_{air}\left[.8 + \frac{T_{dp} - 492}{450}^{1/4}\right] \tag{15}$$

where T_{dp} is the local dew point temperature. Equations 14 and 15 give about the same results at a relative humidity of 25%. The difference between sky and air tempratures range from 20°F in warm moist climates to 50°F in cold dry climates based on Equation 15.

The enclosure that the finned section of an isolated thermosyphon sees includes the upper hemisphere, the sky, and the lower hemisphere, and the ground (snow) surface. As a result, the radiant temperature of the enclosure is approximately the mean temperature of these two bounding surfaces. Table 3, page 16, gives the infrared emmissivity and solar absorptivity data of several surface treatments. A high surface emmissivity will yield a higher radiant heat transfer coefficient. A low solar absorptivity will result in a lower fin surface temperature when solar radiation is incident on the finned surface. Ideally, a surface should have a high infrared emmissivity and a low solar absorptivity.

TESTS

An atmospheric wind tunnel was built and placed in a cold room (temperatures to -22°F) at the U.S. Army Cold Regions Research and Engineering Laboratory (CRREL) at Hanover, New Hampshire (Figure 18). The tunnel is 16 ft long and has an exit section of 4 ft x 8 ft. The tunnel contains eight fans capable of producing air speeds up to 14 mi/hr. Air speeds at the exit section were determined with a calibrated hot wire anemometer. Measurements taken at 0.6 ft intervals along the 8.0 ft height showed a variation in air speed of about 5%.

The schematic of the test setup (Figure 19) shows the condenser section of the thermosyphon in the air stream. The evaporator section was installed in an insulated pipe filled with ethylene glycol and water. Immersion heaters were placed in the fluid to provide a heat source. A circulating pump was installed in the bottom of the pipe to keep the fluid well mixed and to reduce temperature gradients in the fluid along the length of the evaporator. Temperature variation in the fluid along the pipe was typically less than 3.0°F. Four thermocouples were attached to the evaporator section of the thermosyphon and three in the air flow for determining the overall temperature difference. Readings from these thermocouples were averaged to determine the air and evaporator temperatures. Power supplied to the fluid by immersion heaters was measured by use of current and voltage transducers which had DC voltage outputs proportional to the line AC amperes and voltages, respectively. The output from the thermocouples and transducers was connected to a Hewlett Packard data logger.

The thermosyphons used in this study were full-size, commercial, two-phase units. A CO_2-filled type was purchased from Arctic Foundations Inc., Anchorage, Alaska. It had an evaporator section of 2-in nominal pipe, 20-ft long, followed by a 3-ft length of 2-in nominal steel pipe for making the bend, and was then joined to the condenser section by a 3-in x 2-in reducer. The condenser section was 6.8 ft long (8-ft nominal) and consisted of a 3.07-in I.D. and 3.50 in O.D. pipe with segmented annular fins (Figure 15) of rectangular profile oriented horizontally. Dimensionally, the fins were 1.2-in long, 0.3-in wide and 0.049-in thick prior to coating, and had an average spacing of 0.25 in.

Figure 18. Atmospheric wind tunnel with CO_2 thermosyphon.

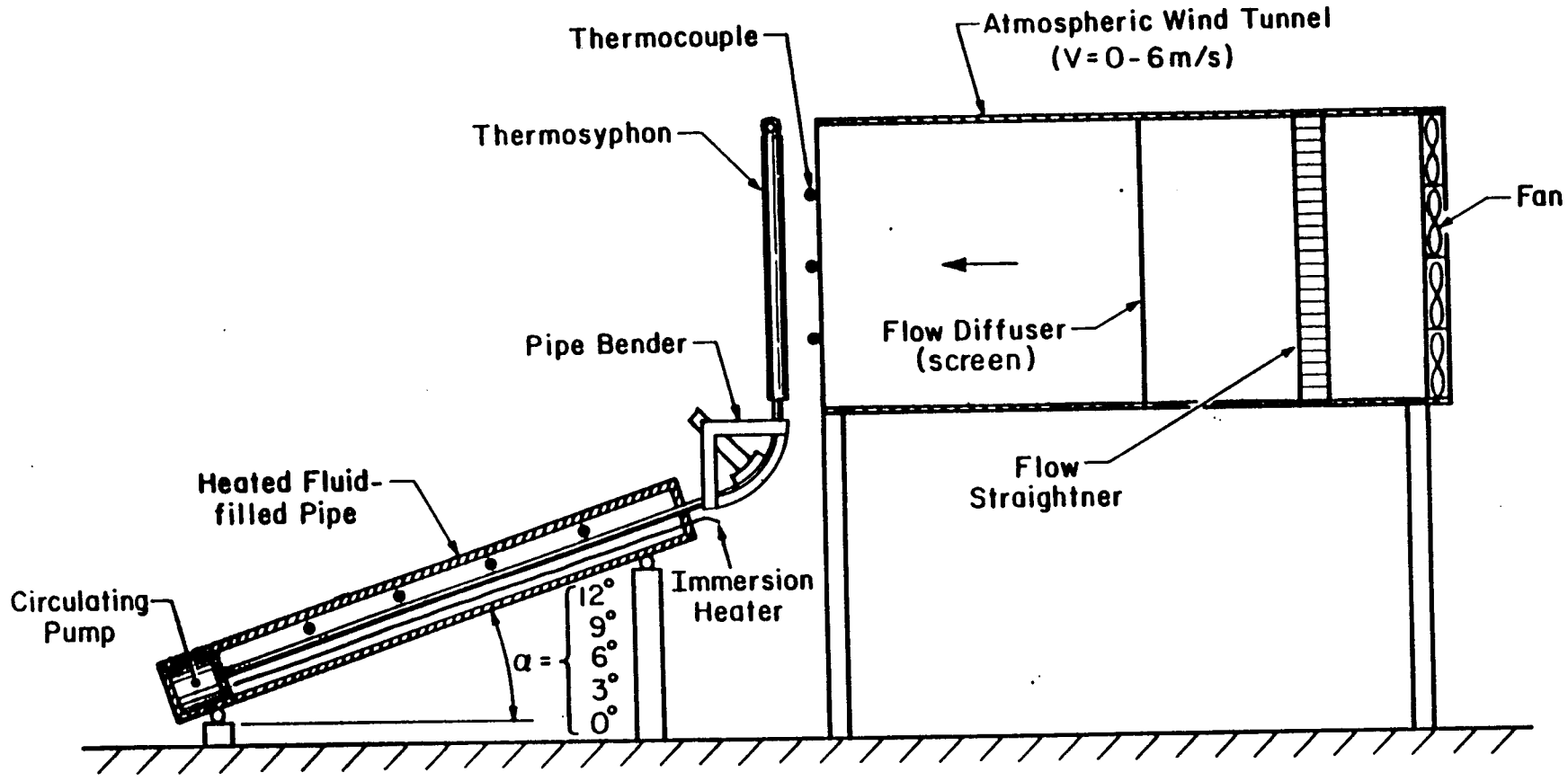

Figure 19. Test setup schematic.

Figure 20 shows a cross section of the extruded anodized aluminum fins supplied on the Cyro-Anchor unit supplied by Mobile Augers and Research Ltd., Edomonton, Alberta. Twenty equally spaced vertical fins 0.125 inches thick extend radially 3.5 inches. The length of the finned area on the condenser section was nominally 8 feet. A 3-foot bendable section and a 20-foot evaporator section comprised the remainder of this thermosyphon.

The maximum initial angle of the 20-foot evaporator section ranged from 9° to 12° from the horizontal, depending on the unit tested (Figure 19). Data were collected with a data logger controlled by a computer, and scans were taken at 10-minute intervals for a hard copy printout. The data were also stored on floppy disks. All tests were conducted at 3°F air temperature. A typical test sequence involved turning on the immersion heaters, circulating pump, and fans. Data were monitored until a steady state (no temperature change) was reached. The steady-state condition was typically reached in about five hours.

After data were obtained at least three different air speeds (0, 8.5 mi/hr and 12.8 mi/hr) for a given evaporator angle, the thermosyphon was bent to a new angle. Data were obtained at five angles, with angles of 6° and 3° representing slopes of 1:10 and 1:20, respectively.

TEST RESULTS

The test data were analyzed to determine the heat removal performance (conductance) of the thermosyphon as a function of inclination angle and air speed. The heat transferred by the thermosyphon was determined by performing an energy balance on the fluid filled pipe. Subtracting the rate of heat loss through the insulation of the fluid filled pipe from the input power yields the heat transfer rate of the thermosyphon. The thermosyphon conductance was then calculated as the thermosyphon heat transfer rate at steady-state divided by the evaporator temperature air temprature difference, or

$$C = \frac{Q}{\Delta T}$$

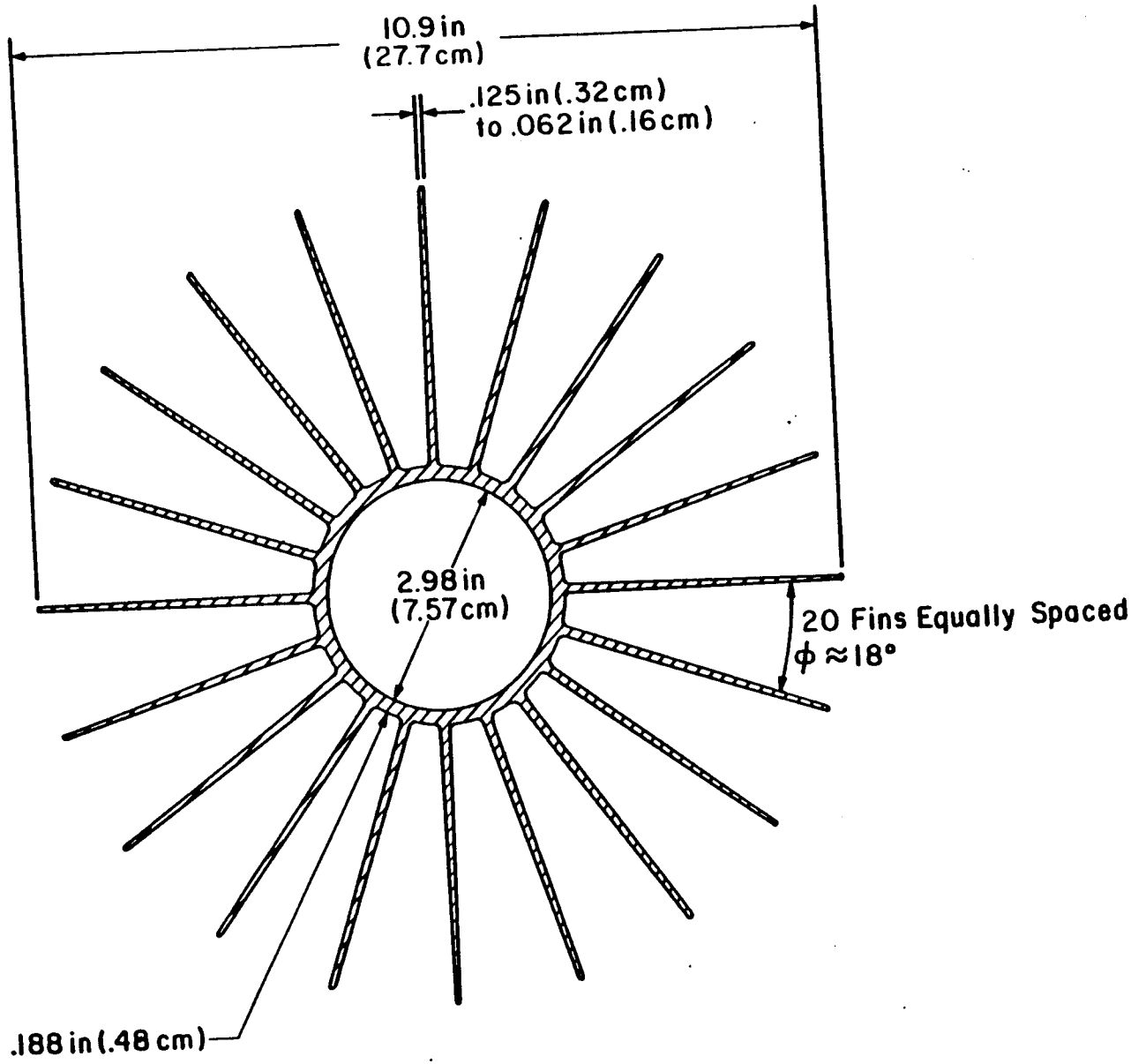

Figure 20. Finned condenser of Cryoanchor.

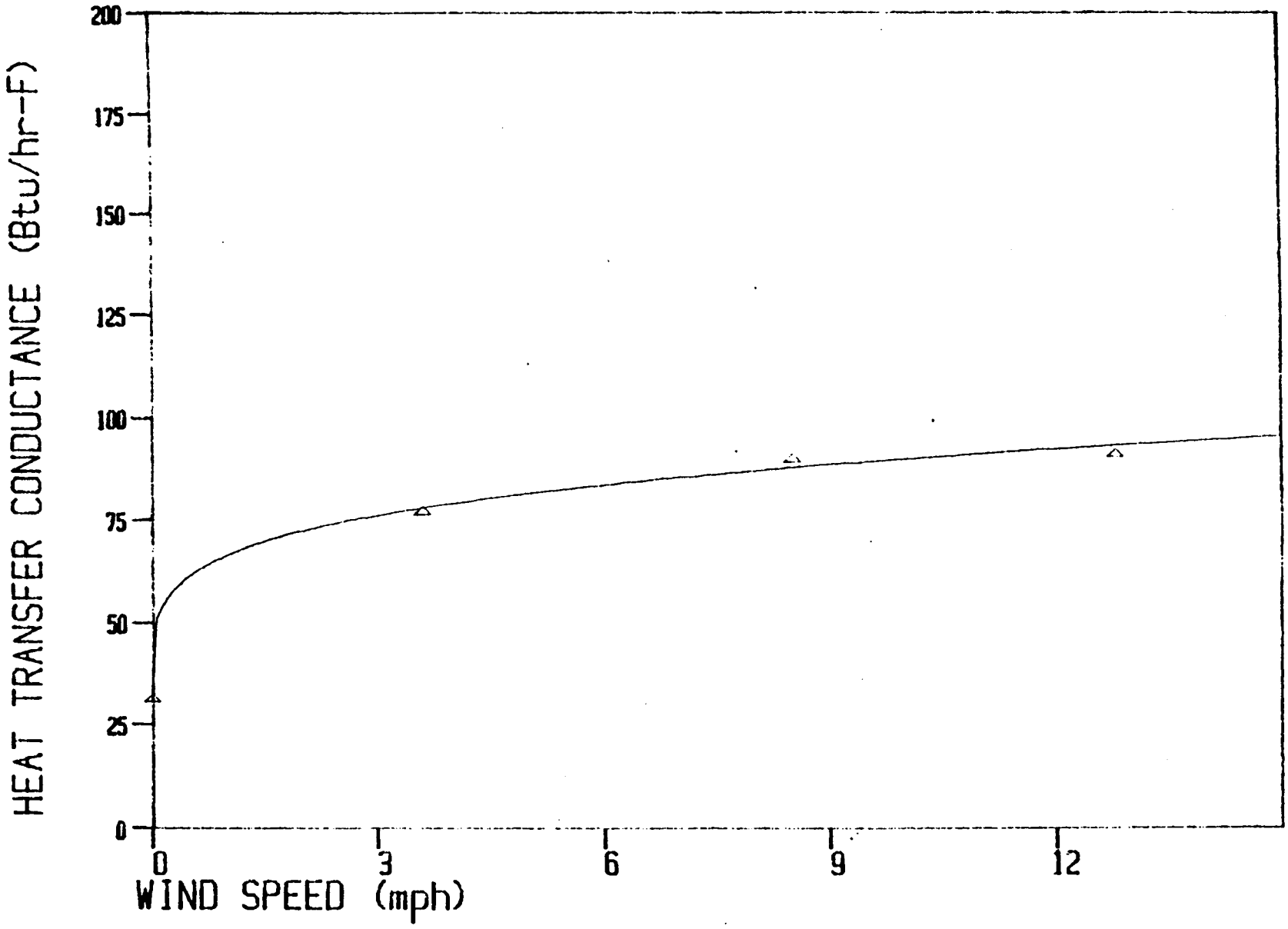

Figure 21. CO_2 thermosyphon (0 degrees tilt).

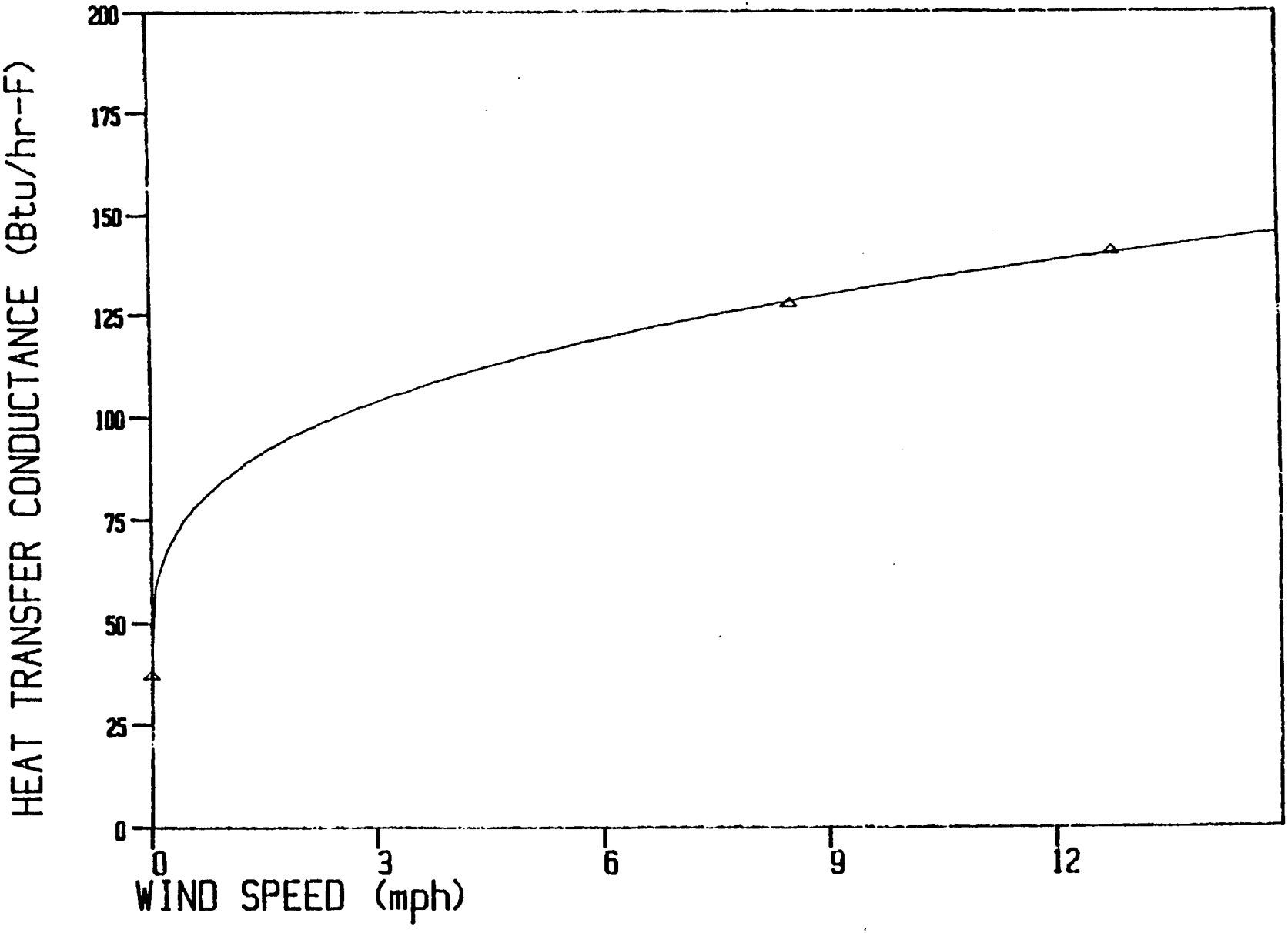

Figure 22. CO_2 thermosyphon (3 degrees tilt).

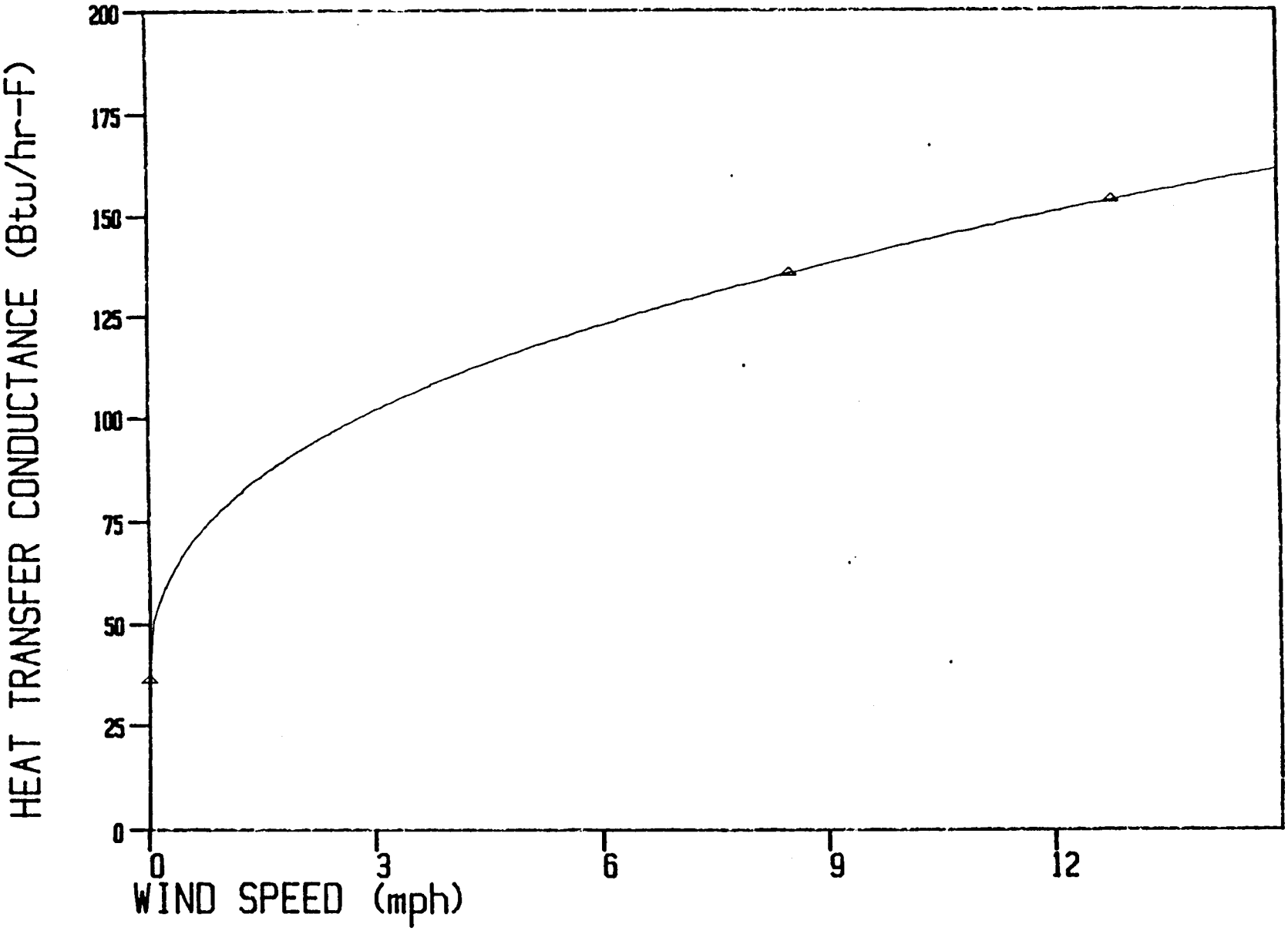

Figure 23. CO_2 thermosyphon (6 degrees tilt).

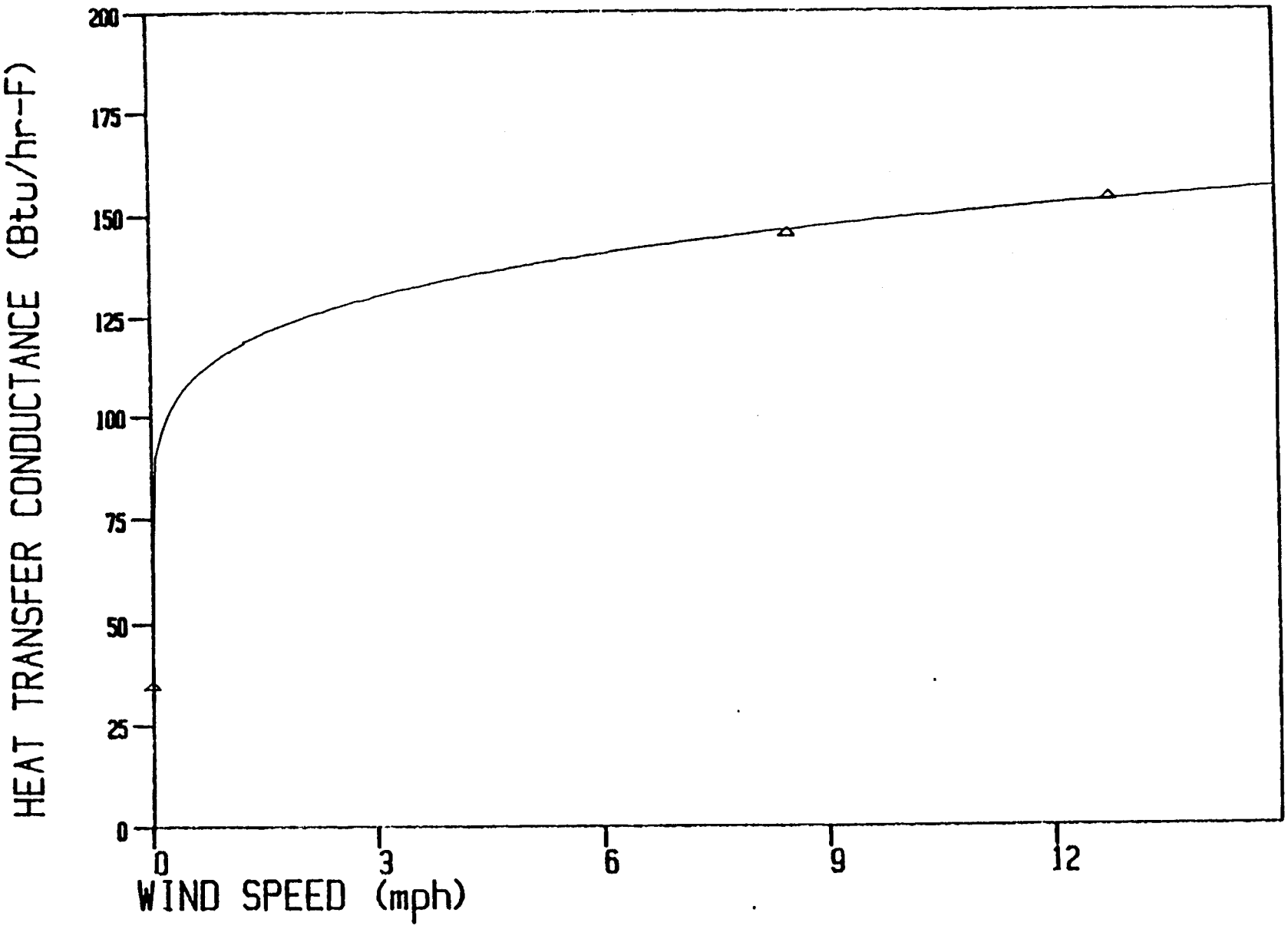

Figure 24. CO_2 thermosyphon (9 degrees tilt).

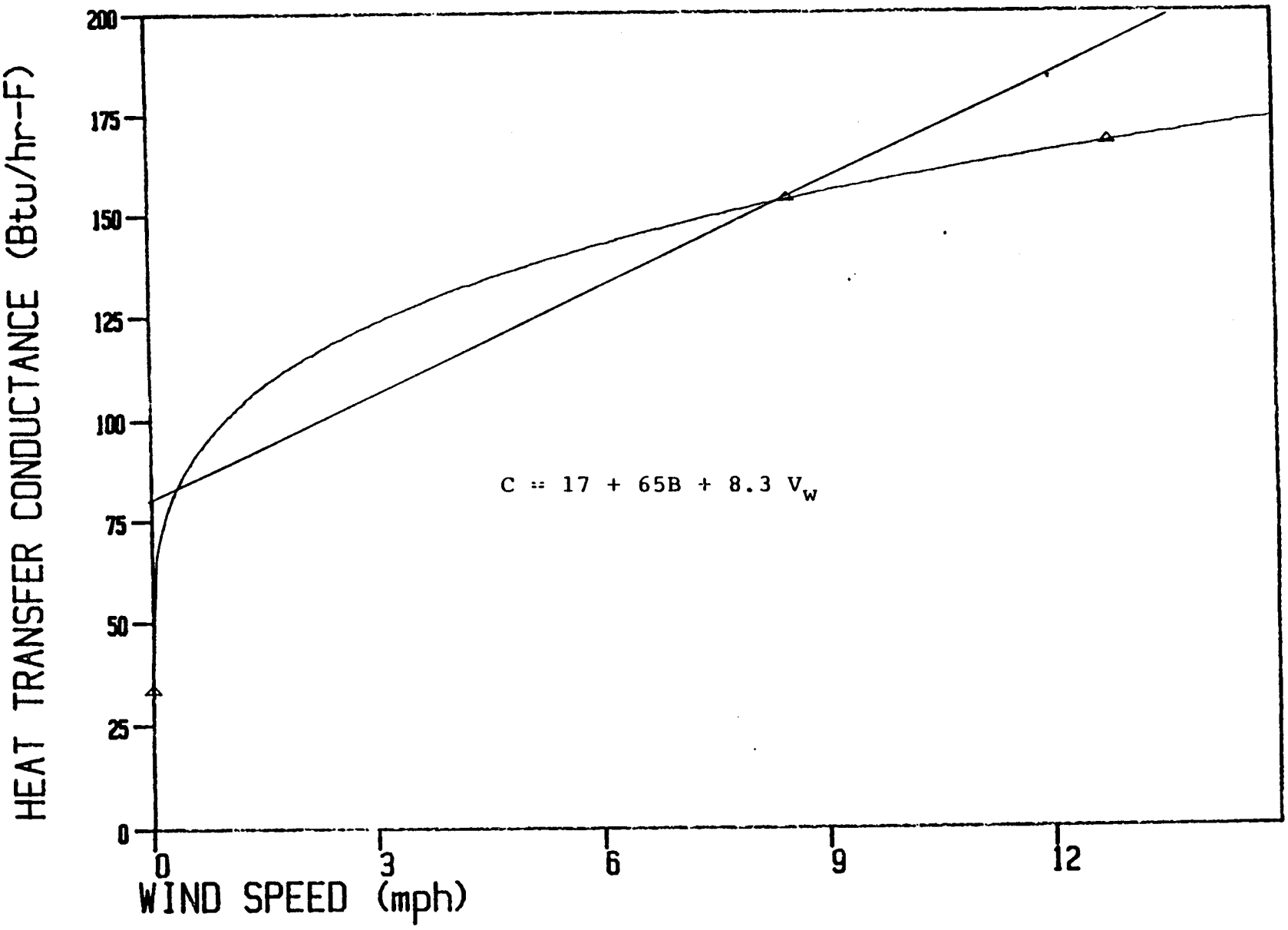

Figure 25. CO_2 thermosyphon (12 degrees tilt).

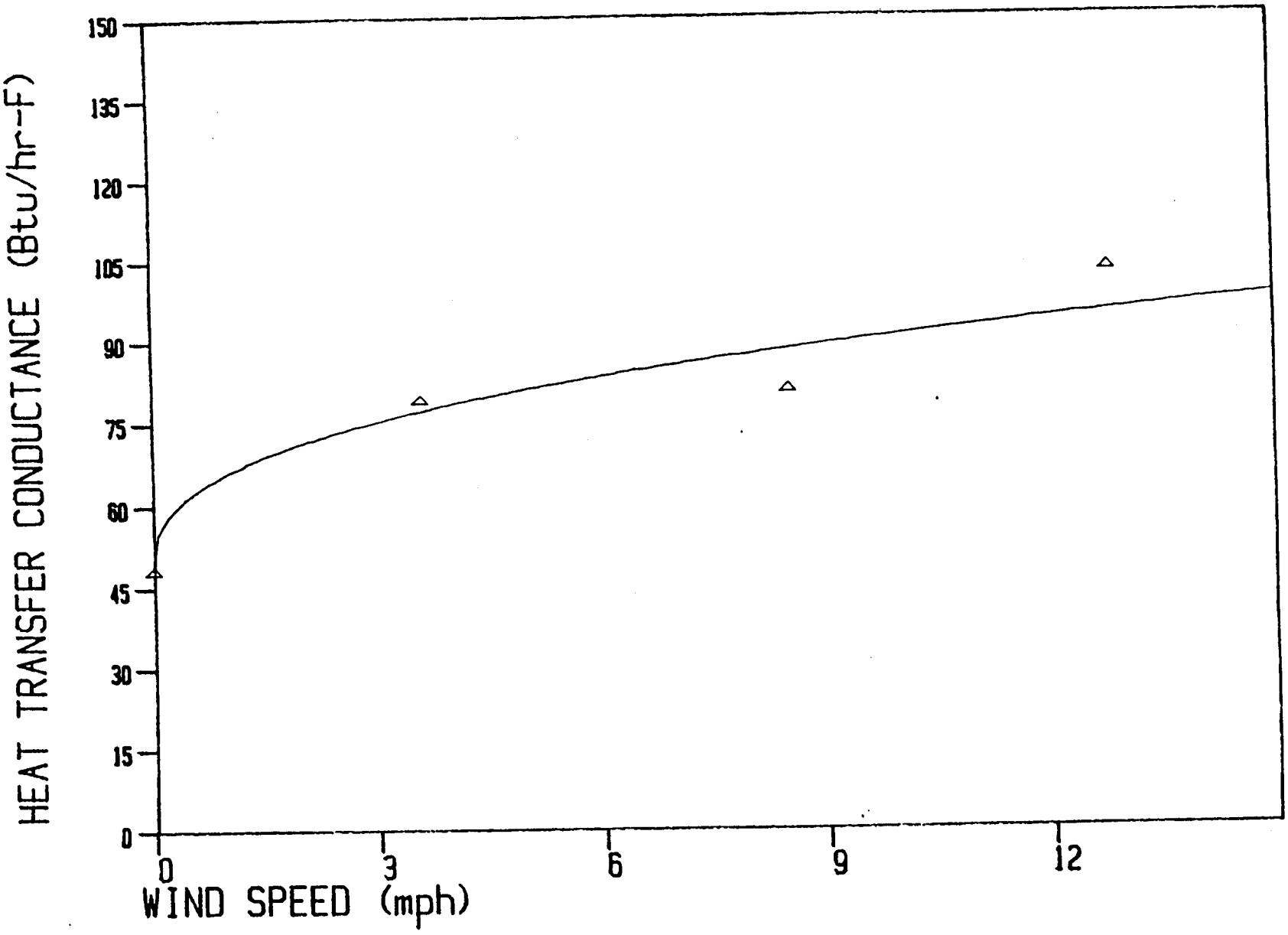

Figure 26. NH_3 thermosyphon (0 degrees tilt).

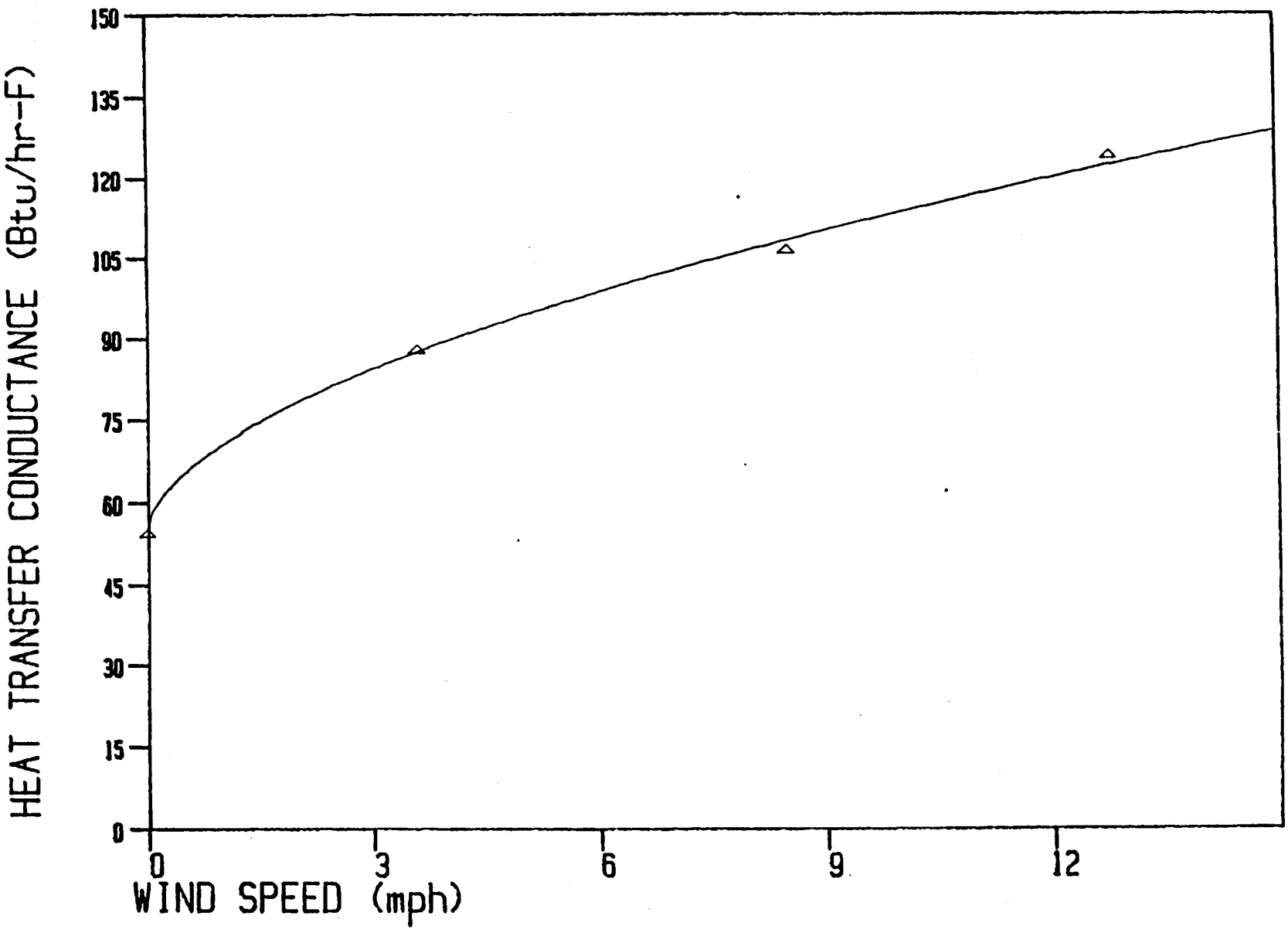

Figure 27. NH_3 thermosyphon (1.5 degrees tilt).

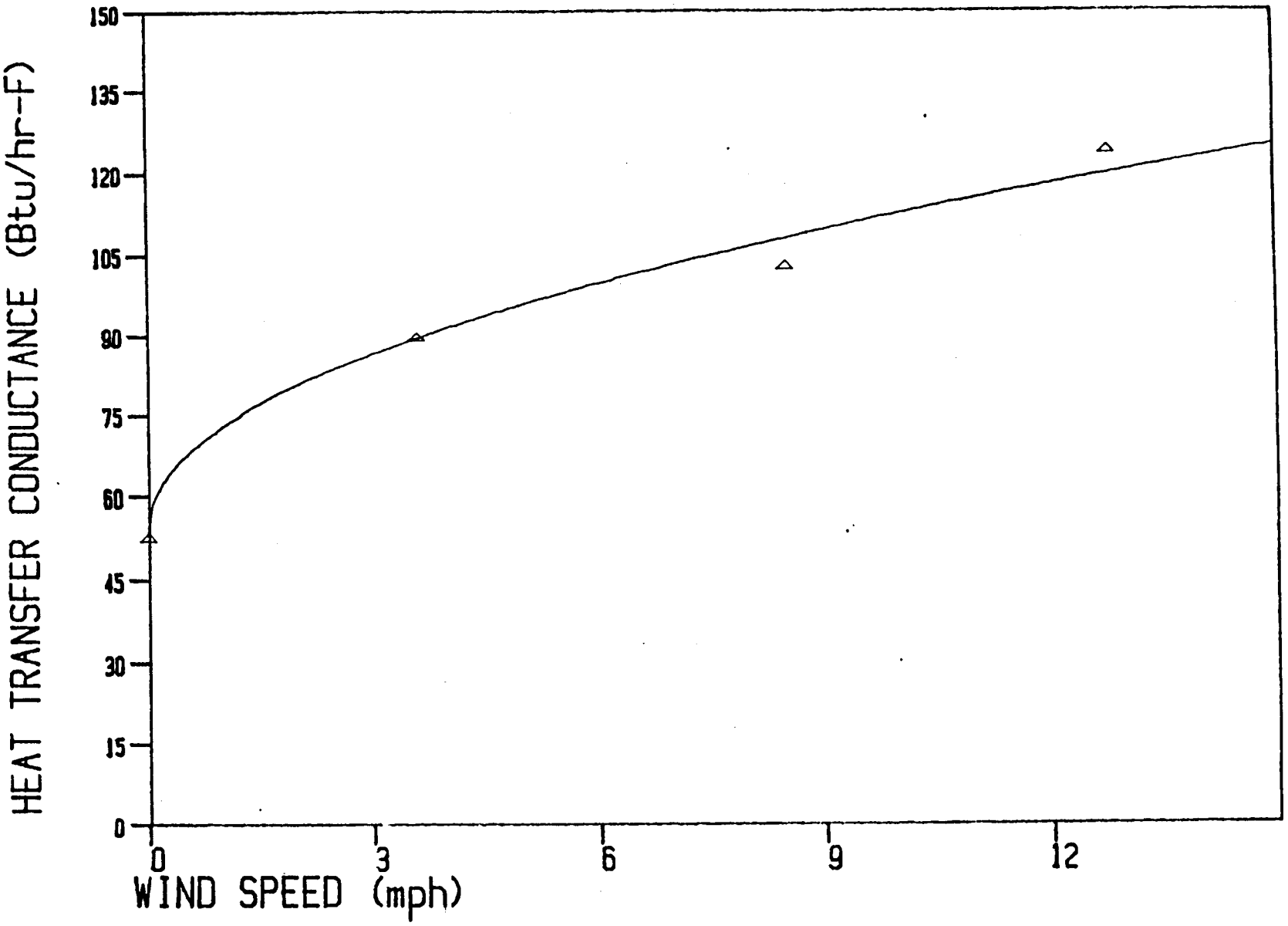

Figure 28. NH_3 thermosyphon (3 degrees tilt).

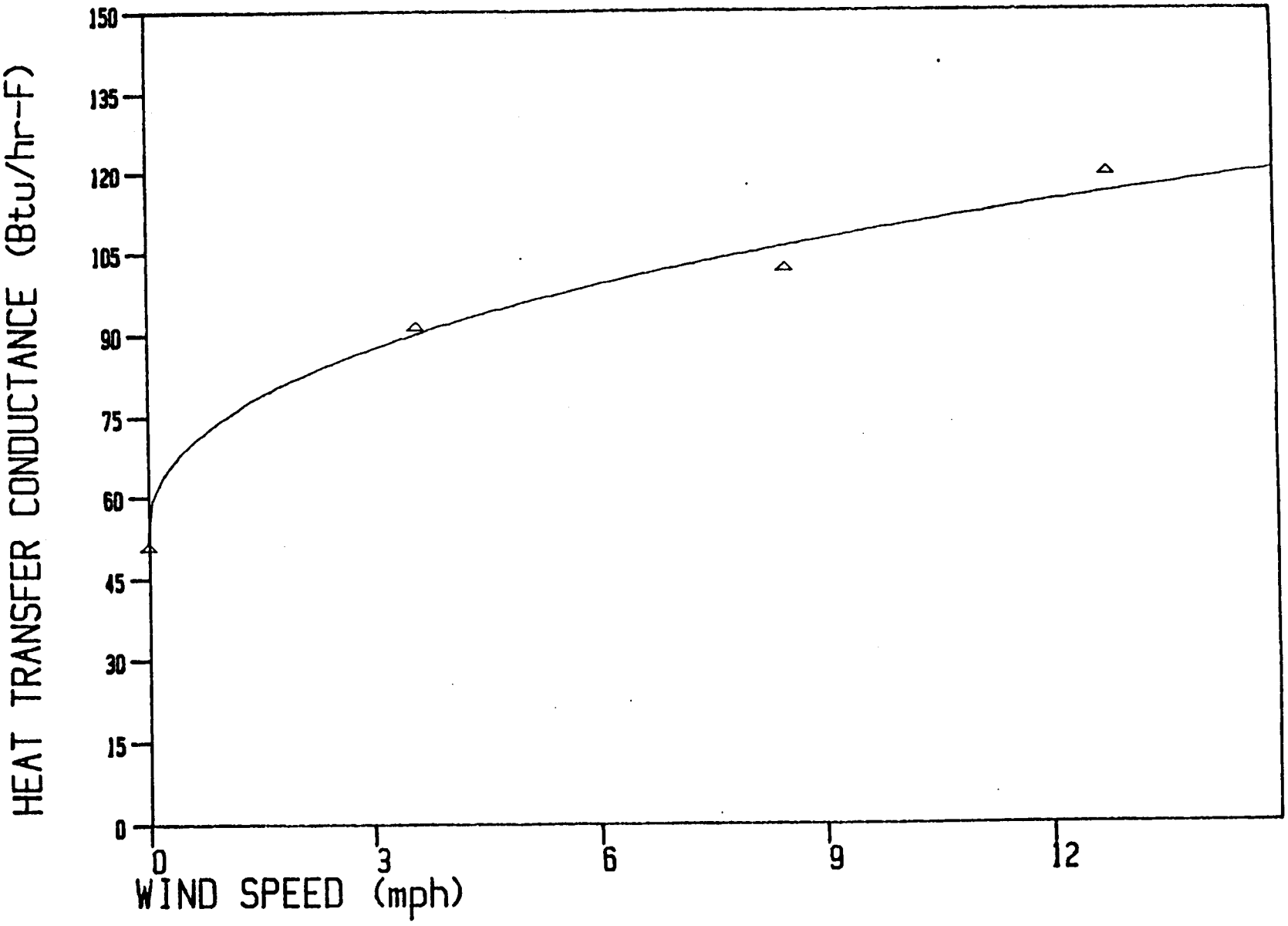

Figure 29. NH_3 thermosyphon (4.5 degrees tilt).

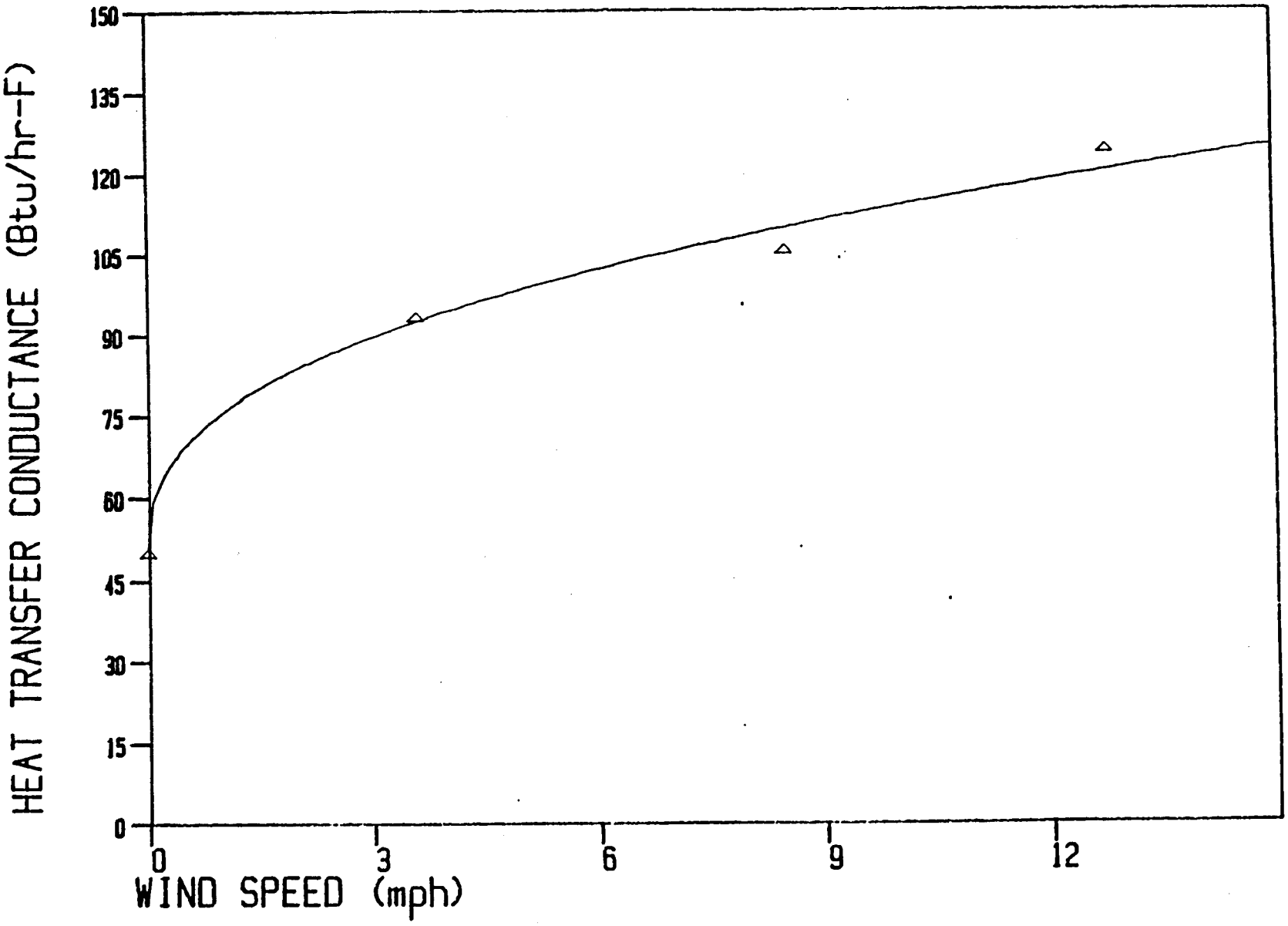

Figure 30. NH_3 thermosyphon (6 degrees tilt).

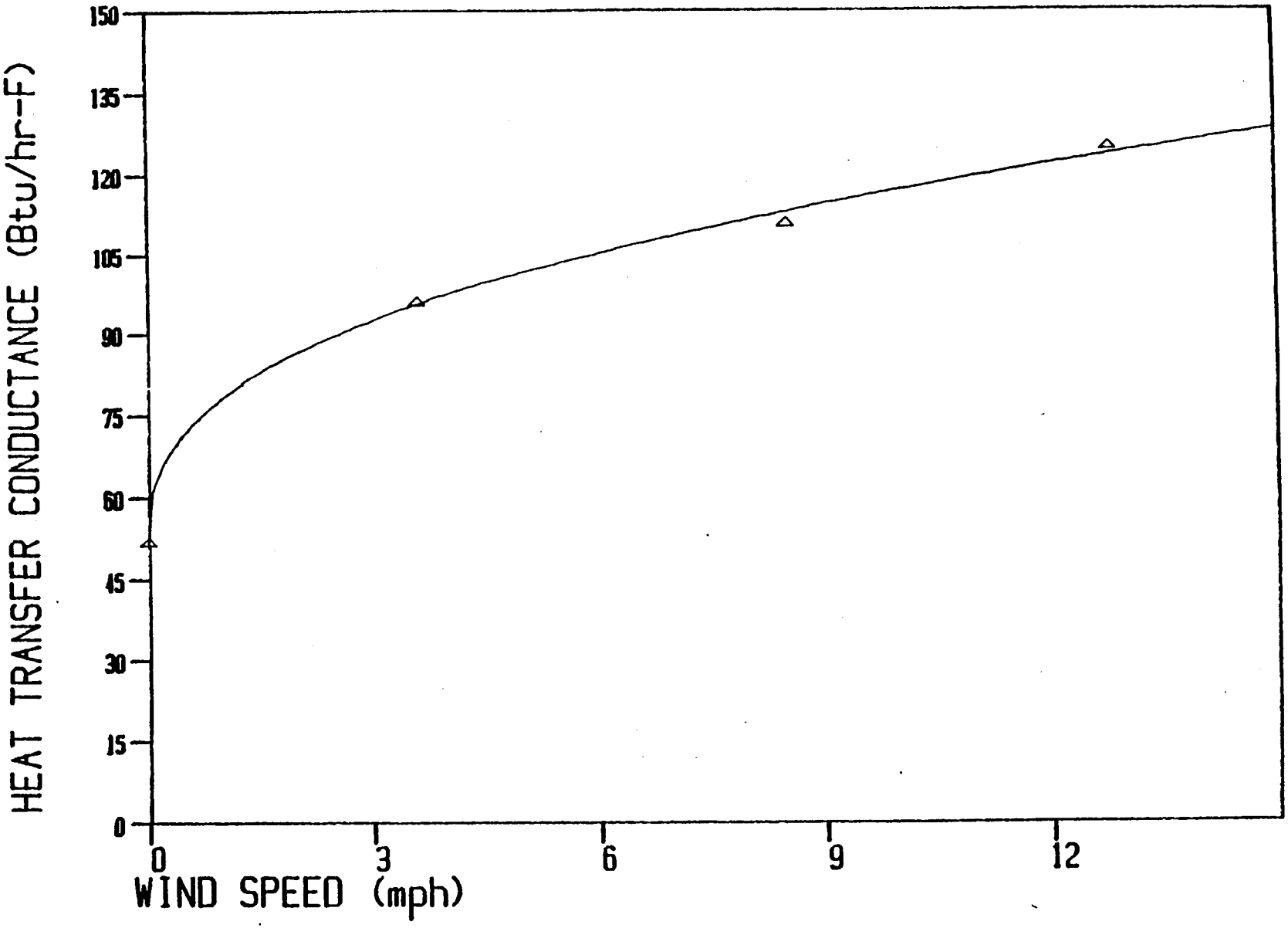

Figure 31. NH_3 thermosyphon (9 degrees tilt).

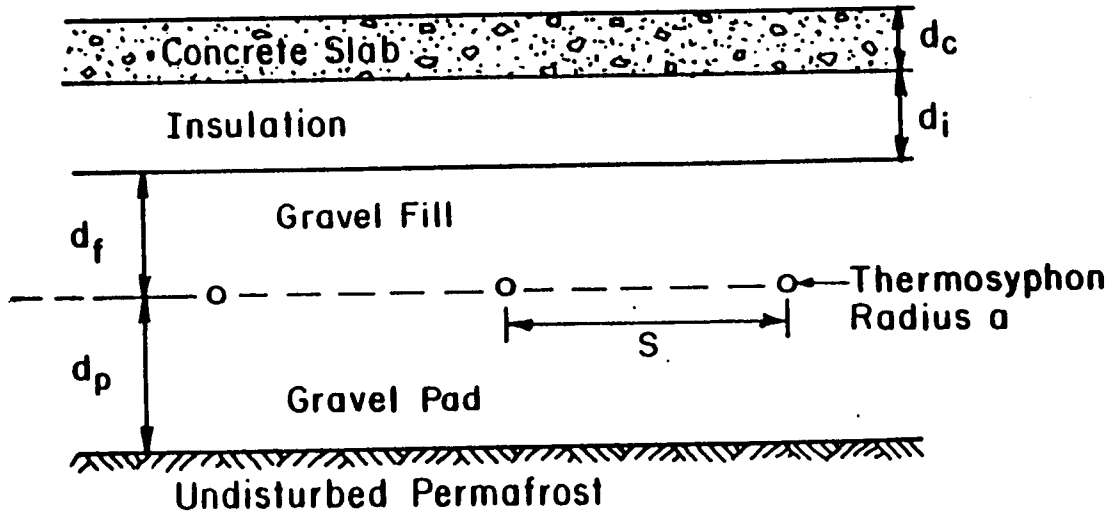

Figure 32. Section of building foundation system using thermosyphons.

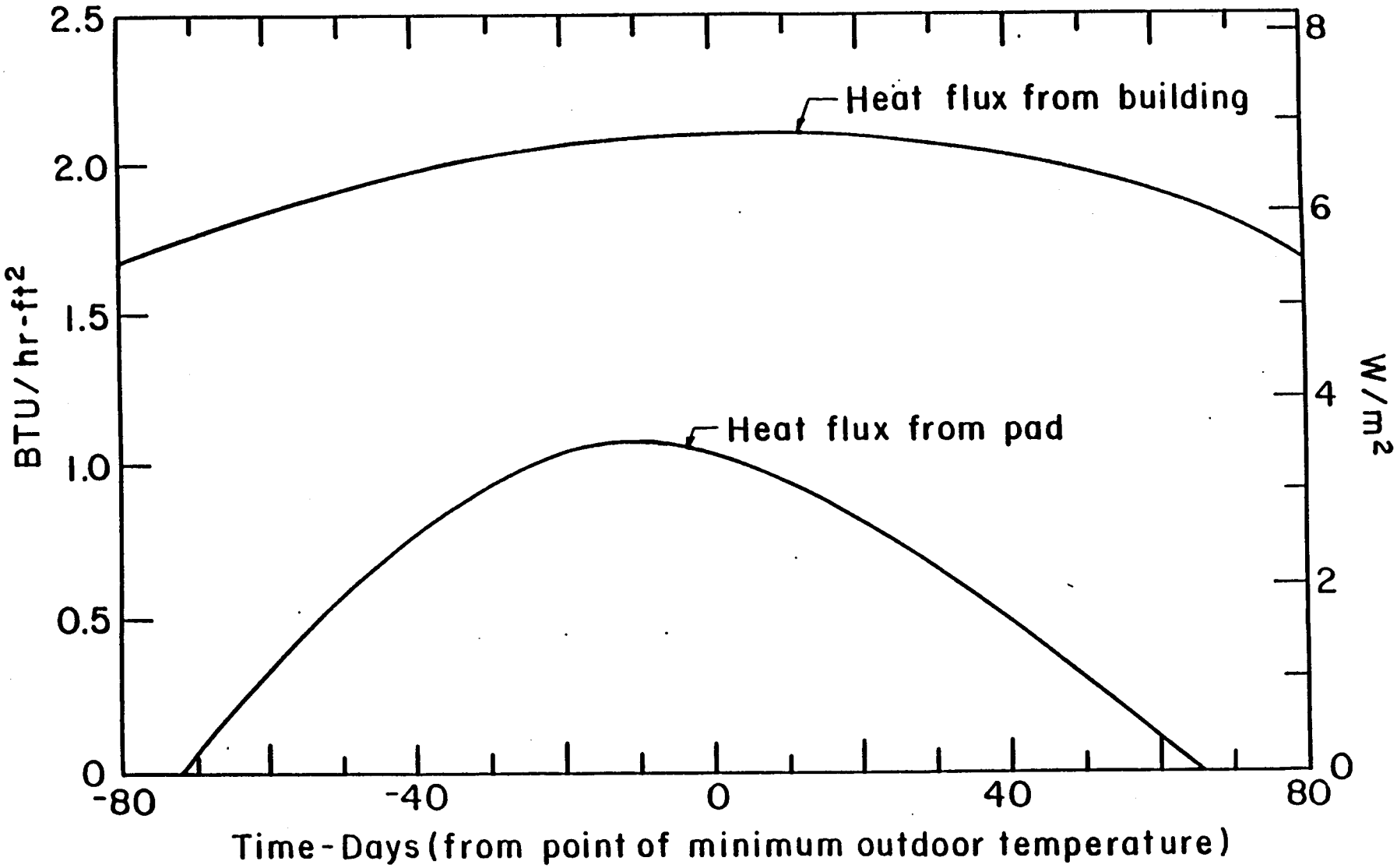

Figure 33. Heat gains from slab and pad to thermosyphon.

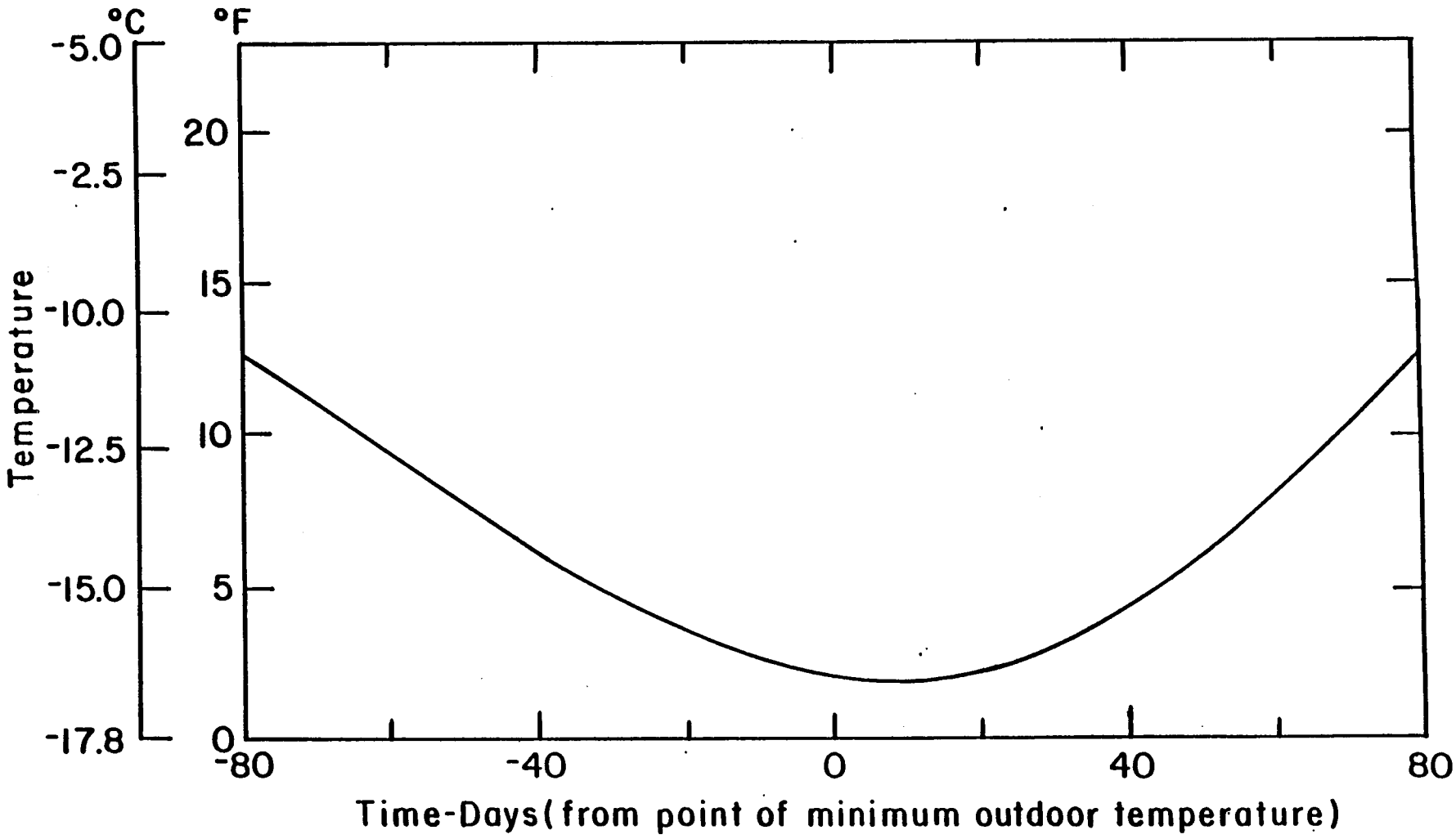

Figure 34. Evaporator temperature as a function of time.

A plot of the overall heat transfer conductance is shown in Figures 21 through 31. These plots indicate a nonlinear relationship between the heat transfer conductance and the wind speed for each of the inclination angles. It should be noted that each datum point represents about six readings, since data were recorded for about an hour after steady state was reached. A logarithmic least squares analysis was used to determine the equations given in Table 4. More data at other air speeds are required to firmly establish these relationships. However, the excellent correlation coefficients and the similarity with other empirical equations for predicting convective heat transfer provides confidence in these relationships.

The fans in the wind tunnel only have two speeds, which limited the data to the wind speeds shown. Present plans provide for a variable frequency drive for the fan motors so that any air speed up to the maximum can be achieved. For the inclination angle of 0°, an extra datum point was obtained a 2.4 mi/hr by turning on only four of the eight fans. The variation in the exit velocity profile from the tunnel increased from 5% to about 27% for this datum point. However, this point was plotted because it confirms the relationship found with the other data.

Results of the tests show that the heat transfer conductance increases with wind speed and inclination angle. The results of this study agree with laboratory work done by Lee and Bedrossian (1978) and Negishi and Sawada (1983). They did tests with small thermosyphons at inclined angles. Negishi and Sawada found a considerable decrease in the heat transfer rate at an inclination angle of 0°. They observed a dry-out phenomenon in the evaporator where the condensate did not reach the bottom of the tube before being evaporated. Our data generally agree with theirs.

Arctic Foundations Inc. have provided an empirical expression for the heat transfer rate of their unit (Yarmak, 1983). Their linear relationship for any evaporator angle is

$$C = 9.0 + 34.3B + 9.8\ V_w \qquad [W/°C] \qquad (16)$$

or

TABLE 4. Empirical expressions for overall heat transfer conductances.

Angle of evaporator	S.I. [W/°C]	English [Btu/hr-°F]
CO_2 Thermosyphon		
0	$16.8+22.0V^{.226}$	$31.8+34.6V^{.226}$
3	$19.6+32.4V^{.300}$	$36.9+48.1V^{.300}$
6	$19.0+31.0V^{.400}$	$35.9+42.4V^{.400}$
9	$18.9+47.9V^{.150}$	$35.7+80.2V^{.150}$
12	$17.8+43.8V^{.275}$	$33.7+66.4V^{.275}$
NH_3 Thermosyphon		
0	$25.6+12.7V^{.384}$	$48.4+17.5V^{.384}$
1.5	$29.0+13.2V^{.572}$	$54.8+15.7V^{.572}$
3.0	$28.0+15.4V^{.476}$	$52.9+19.9V^{.476}$
4.5	$27.2+16.9V^{.403}$	$51.4+23.1V^{.403}$
6.0	$26.7+18.3V^{.403}$	$50.5+25.0V^{.403}$
9.0	$27.3+19.2V^{.392}$	$51.6+26.5V^{.392}$
where V is air speed	[m/s]	[mi/hr]

$$C = 17 + 65B + 8.3V_w \qquad [Btu/hr\text{-}°F] \qquad (17)$$

where B is a factor based on the exposure of the thermosyphon (B = 1 in open area, B = 0.75 at an outside corner of a building, B = 0.5 next to a building, and B = 0.25 at an inside corner of a building) and V_w is the wind speed. Equation 17 has been plotted on Figure 25 to show the comparison for B equal to 1. Equation 17 overestimates the heat transfer conductance at very low wind speeds and underestimates it at wind speeds above 9 mi/hr compared to the thermosyphon tested at a 12 degree tilt angle.

FOUNDATION DESIGN WITH THERMOSYPHONS

There are many instances in arctic locations when the subgrade consists of permafrost that is not thaw-stable and it is desirable to design a building with a slab-on-grade foundation. This type of foundation design requires insulation below the floor slab to retard the flow of heat and a heat rejection system below the insulation to prevent the thermal degradation of the underlying permafrost. Heat rejection systems that have been used in this application are mechanical refrigeration consisting of a chiller coupled to a grid of pipes or air ducts or thermosyphons placed in the gravel pad below the floor insulation. Figure 32 shows a typical section of a slab-on-grade foundation with thermosyphons installed on a center-to-center spacing, S.

The following analysis could be used early in the design phase for making approximate calculations as to the thermosyphon configuration (spacing) and thermosyphon conductance and insulation thickness needed to protect the underlying permafrost from thaw. Computer models using the finite difference or finite element methods should be used to finalize the design. In this analysis, it is assumed that thermal energy is transferred to the thermosyphon from three sources: (1) latent heat released in the freezing of the gravel fill and pad following the summer thaw, (2) heat transferred through the floor of the building, and (3) heat transferred from the underlying permafrost up

through the pad. The analysis is quasi-steady as it generally neglects sensible energy storage in the concrete slab, insulation, and gravel fill and pad, but it includes the sensible energy stored in the underlying permafrost. The per unit length conductance of the thermosyphon, C*, is divided into C_1*, C_2*, C_3* which are sized to meet the three loads already outlined.

The outdoor ambient air temperature is assumed to vary sinusoidally with a mean value T_m and an amplitude A_o, or

$$T_a = T_m - A_o \cos\left(\frac{2\pi t}{365}\right) \tag{18}$$

where t is the time in days measured for the time the air temperature passes through its minimum value (usually mid-January). To determine the length of the summer thaw season, the right side of equation (18) can be set equal to the freezing temperature and then solved for the values of t_1 and t_2. These two values of time represent the first day the outdoor temperature rises above the freezing temperature and the last day the outdoor temperature remains above the freezing temperature:

$$t_1,\ t_2 = \frac{365}{2\pi} \cos^{-1}\left(\frac{T_m - T_f}{A_o}\right) \tag{19}$$

The difference between t_1 and t_2 represents the length of the summer thaw season. It may be desirable to choose a temperature below freezing to provide a margin of safety for a long, warm summer. The depth of thaw or minimum thickness of gravel required to contain the summer thaw and prevent the thaw of the underlying permafrost can be calculated based on a quasi-steady analysis, similar to one given in Harlan and Nixon (1978) or

$$d_f + d_p = -(R_c+R_i)K_g + \{K_g^2(R_c+R_i)^2 + 2K_gL^{-1}(T_s-T_f)(t_2-t_1)\}^{1/2} \tag{20}$$

where

d_c = thickness of concrete slab
d_i = thickness of insulation
d_f = thickness of fill
d_p = thickness of pad
R_c = thermal resistance of concrete slab, (d_c/K_c)
R_i = thermal resistance of insulation, (d_i/K_i)
K_c = thermal conductivity of concrete
K_i = thermal conductivity of insulation
K_g = thermal conductivity of gravel
L = latent heat of gravel
T_s = floor temperature of building
T_f = freezing temperature

This depth can be reduced by the factor (1 - Ste/8), as given in Harlan and Nixon (1978), which accounts for the changes in sensible energy in the gravel that Equation 20 neglects. If this factor is applied, the Stefan Number, Ste = C'ΔT'L, should be defined based on the difference between the temperature at the top of the gravel fill and the freezing temperature. Conservatively, this can be chosen as the average temperature difference for the summer thaw season. C' is the volumetric specific heat of the thawed gravel.

An equivalent radius of the zone of material to be frozen back during the winter season can be estimated for designs in which the thermosyphon is approximately centered in the gravel pad, and fill and S are not significantly greater then $d_f + d_p$ as

$$r_f = \sqrt{S(d_p + d_f)/\pi} \tag{21}$$

This radius can be increased to account for the nonsteady temperature distribution by applying the Pekeris and Slicher (1939) factor, or

$$r_f' = r_f(1 - .12\ \text{Ste})^{1/2} \tag{22}$$

where Ste is the Stefan Number, C'ΔT*/L. In this case ΔT* is the difference in temperature between freezing and average thermosyphon

evaporator temperature during winter. C' is the volumetric specific heat of frozen gravel.

The conductance, C_1^*, of the thermosyphon needed to freeze an area of soil radius, r_f', can be derived from a relationship presented by Haynes and Zarling (1982):

$$C_1^* = \left[\frac{F.I.}{\pi L(r_f'^2 - a^2)} + \frac{1}{4\pi K_g} - \frac{r_f'^2 \ln(r_f'/a)}{2\pi K_g (r_f'^2 - a^2)}\right]^{-1} \qquad (23)$$

where

F.I. = local freezing index
K_g = thermal conductivity of frozen gravel

The total heat flux per thermosyphon spacing, S, from the building that is transferred through the floor slab, insulation and gravel fill to the thermosyphon and finally to the outdoor air is

$$Q = \frac{(T_s - T_a)}{(R_c + R_i + R_f)/S + 1/C_2^*} \qquad (24)$$

where

T_s = floor surface temperature
T_a = ambient air temperature
C_2^* = portion of thermosyphon conductance required to meet heat gain from structure
R_c = thermal resistance of concrete floor slab
R_i = thermal resistance of insulation
R_f = termal resistance of gravel fill

$$R_f = S\{\ln[\frac{S}{\pi a}\sinh(\frac{2\pi d_f}{S})] + \cosh^2(\frac{2\pi d_f}{S})/$$

$$[1 - (\frac{1}{3} + \frac{S^2}{\pi^2 a^2})\sinh^2(\frac{2\pi d_f}{S})]\}/2\pi Kf \qquad (25)$$

The expression for the thermal resistance of the gravel fill is based on the geometrical shape factor equation given by Caulk (1983). This shape factor is for an infinite row of holes of radius, a, spaced S on center and at a depth, d_f.

The temperature distribution in a semi-infinite region of ground with a surface resistance subjected to a sinusoidal air temperature variation is given in Meyers (1971) as

$$T(x,t) = T_m - A_o \frac{e^{-x\sqrt{\pi/365\alpha}}}{(\gamma+1)^2 + \gamma^2} \cos\left(\frac{2\pi t}{365} - x\sqrt{\pi/365\alpha} - \phi\right) \qquad (26)$$

where

$$\phi = \tan^{-1}\left(\frac{\gamma}{\gamma + 1}\right) \qquad (27)$$

and

$$\gamma = \left(\frac{S}{C_3^*} + R_p\right) K_{pf} \sqrt{\pi/365\alpha} \qquad (28)$$

α = thermal diffusivity of permafrost
R_p = thermal resistance of the pad
C_3^* = portion of thermosyphon conductance required to transfer heat load from pad
K_{pf} = thermal conductivity of permafrost.

The heat flux at the base of the pad (top of the undisturbed permafrost) can be determined by taking the derivative of equation (28) with respect to x at the permafrost surface (x = 0) or

$$Q = \frac{S\, A_o\, K_{pf} \sqrt{\pi/365\alpha}}{(\gamma+1)^2 + \gamma^2} \left[\cos\left(\frac{2\pi t}{365} - \phi\right) - \sin\left(\frac{2\pi t}{365} - \phi\right)\right] \qquad (29)$$

The pad thermal resistance, R_p, is calculated using equation (25) for R_f, except K_f and d_f are replaced with K_p and d_p.

The equations presented for the heat fluxes from the building and the permafrost to the thermosyphon do not result in closed form solutions for the conductances C_2^* and C_3^*. Therefore, an iterative

solution must be used to arrive at a balanced design where the temperature of the thermosyphon evaporator is the same for both the building heat gain and the pad heat gain solutions. This iterative solution is best carried out on a digital computer. The results are presented for the example case are the output from an IBM-PC microcomputer on which the equations in this analysis were programmed.

A thermosyphon with a per unit length conductance of 1.2 Btu/hr-ft-F° was used for the foundation of a building heated to 70°F is shown in Figure 32 and described in Table 5. The thermosyphons are placed 8 ft on center and have a diameter of 0.25 ft. The building site is Barrow, Alaska, with a freezing index of 8,500 F° days, a mean annual temperature of 9°F and a seasonal temperature variation of 32 F°.

Using the analysis we've outlined for the sample problem described yields the following results. The equivalent radius of gravel to be frozen back is 3.4 ft, which yields a conductance C_1^* = 0.2 Btu/hr-ft-F°. This results in a conductance $C_2^* + C_3^*$ = 1.0 Btu/hr-ft-F° available to transfer the building slab and pad heat gains to the thermosyphon. Figure 33 shows the building slab and pad heat gains to the thermosyphon. Because of the time-varying nature of these loads, C_2^* and C_3^* also vary with time; however, their sum remains constant at 1.0 Btu/hr-ft-°F for this example. Finally, the evaporator temperature as a function of time is presented in Figure 34. Equation 23 is used to calculate this temperature at x equals zero.

CONCLUSIONS

The performance of the two thermosyphons tested in this project decreased as the angle of their evaporator sections approached horizontal. Therefore, vertical conductance values must be downgraded when designing systems using thermosyphons with inclined evaporator sections.

The two thermosyphons tested in this project differed in performance. This difference is mainly due to the different fin configurations used on the competing units. The CO_2-filled unit with horizontal fins supplied by Arctic Foundations yielded superior

TABLE 5. Properties of foundation and materials in example.

Concrete

$d_c = 0.5$ ft
$T_s = 70°F$
$K_c = 1.0$ Btu/hr-ft-F°

Insulation

$d_i = 0.50$ ft
$K_i = 0.17$ Btu/hr-ft-F°

Fill and pad

$d_f = 2$ ft
$d_p = 2$ ft
$L_f = L_p = 1{,}170$ Btu/ft^3
$C'_p = C'_f = 36.4$ Btu/ft^3-F°(frozen)
$C'_p = C'_f = 45.1$ Btu/ft^3-F° (thawed)
$K_f = K_p = 2.3$ Btu/hr-ft-F° (frozen)
$K_f = K_p = 1.7$ Btu/hr-ft-F° (thawed)

Permafrost

$K_{pf} = 1.0$ Btu/hr-ft-F°
$c'_{pf} = 40$ Btu/ft^3-F°

performance under windy conditions. However, the ammonia-filled unit with vertical fins (supplied by Mobile Augers and Research Ltd.) had a higher conductance under still air conditions. Arctic Foundations' unit has a considerably lower purchase cost which gives it a competitive edge, all else being equal.

Finally, a preliminary design methodology has been presented for sizing and selection of thermosyphon units and configuration for on-grade systems. We recommend finite difference or finite element techniques for final design.

ACKNOWLEDGMENTS

Erv Long of Arctic Foundations, Anchorage, Alaska, provided some of the material in the working fluid and container sections in the body of this report as well as supplying several photographs. His helpful discussions, information and critque are deeply appreciated. The authors also acknowledge the assistance of the secretaries, technicians and students who all participated in this project in one manner or another to bring it to completion.

REFERENCES

ASHRAE. 1981. Handbook of Fundamentals. American Society of Heating, Refrigerating and Air Conditioning, Atlanta, GA. pp. 16-1 - 17-72.

Babb, A.L., D.M. Chow, K.L. Garlid, R.P. Popovich and E.M. Woodruff. 1971. The thermo tube, a natural convection heat transfer device for stabilization of arctic soils in oil producing regions. Soc. of Pet. Engrs. Paper No. SPE 3618. 12 pp.

Babb, A.L., A. Godal, A.W. Wakefield, R.E. McKee and M.J. Strand. 1978. A natural circulation self-refrigerated pile for direct support of buildings in permafrost regions. A.I.Ch.E. Symposium Series. 174(74):223-234.

Balch, J.C. 1968. Soil Refrigeration Systems. U.S. Patent 26387. 5 pp.

Barthelemy, J.L. 1980. Performance of a natural convection heat exchange system for subgrade cooling of permafrost. Pages 235-261 in Building under Cold Climates and on Permafrost. U.S. Army Corps of Engineers, Port Hueneme, CA.

Basiulis, A., and R.C. Prager. 1975. Compatibility and reliability of heat pipe materials. Pages 515-529 in AIAA 10th Thermophysics Conference, Denver, CO. Paper No. 75-660.

Briggs, D.E., and E.H. Young. 1963. Convection heat transfer and pressure drop of air flowing across triangular pitch banks of finned tubes. Chemical Engineering Progress Symposium Series. 59(41):1-9.

Caulk, D.A. 1983. Steady heat conduction from an infinite row of holes in a half space or a uniform slab. Int. J. Heat and Mass Transfer. 26(10):1509-1513.

Chen, K. 1982. The influence of loop configuration on closed loop thermosyphons. ASME Winter Annual Meeting, Phoenix, AZ. Paper 82-WA/HT-63. 7 pp.

Clements, B., and Y. Lee. 1981. Additional parameters in two-phase closed thermosyphons effects of tube diameter and wall thickness. Int. J. Heat Mass Transfer. 24(9):1554-1555.

Cronin, J.E. 1983. Design and performance of a liquid natural convection subgrade cooling system. Proceedings of 4th International Permafrost Conference, National Academy Press. 1:198-203.

Feldman, K.T. 1967. The heat pipe. Mechanical Engineering, ASME. 89:30-33.

Ferrara, A., and P. Brinkman. 1976. Applying heat pipes to avoid the preferential freezing of highway bridge decks. Intersociety Conference on Environmental Systems, San Diego, CA. ASME Paper No. 76-ENAs-25. 5 pp.

Galate, J.W.. 1976. Passive refrigeration for arctic pile supports. Trans. ASME, J. Engineering for Industry. 98(2):695-700.

Gaugler, G.M. 1944. Heat Transfer Device. U.S. Patent No. 2350348.

Gay, F.W. 1929. Thermosyphon Gas-to-gas Heat Exchanger. U.S. Patent 1725906.

Harlan, R.L., and J.F. Nixon. 1978. Ground thermal regime. Pages in Geotechnical Engineering for Cold Regions. McGraw Hill, NY.

Hayley, D.W. 1982. Application of heat pipes to design of shallow foundations on permafrost. Pages 535-544 Proceedings of the 4th Canadian Permafrost Conference. National Research Council of Canada, Ottawa.

Hayley, D.W., W.D. Roggensack, W.E. Jubien and P.V. Johnson. 1983. Stabilization of sinkholes on the Hudson Bay Railway. Pages 468-473 in Proceedings of 4th International Permafrost Conference. National Academy of Science, Washington, DC.

Haynes, F.D., and J.P. Zarling. 1982. A comparative study of thermosyphons used for freezing soil. ASME Winter Annual Meeting, Phoenix, AZ. ASME Paper No. 82-WA/HT-40. 5 pp.

Heuer, C.E. 1979. The application of heat pipes on the Trans-Alaska pipeline. U.S. Army CRREL, Hanover, NH. Special Report 79-26. 27 pp.

Jahns, H.O., T.W. Miller, L.D. Power, W.P. Rickey, T.P. Taylor and J.A. Wheeler. 1973. Permafrost protection for pipelines. Pages

673-683 in Proceedings of the 2nd International Permafrost Conference, Yakutsk, USSR. National Academy of Sciences, Washington, DC.

Johnson, P.R. 1971. Empirical heat transfer rates of small, long and balch thermal piles and thermal convective loops. Institute of Arctic Environmental Engineering, University of Alaska, Fairbanks. Report 7102. 56 pp.

Lee, Y. 1978. Preservation of permafrost by means of two-phase closed thermosyphon. University of Ottawa, Ontario. Annual Reports, DRB9511-96.

Lee, Y., and A. Bedrossian. 1978. The characteristics of heat exchangers using heat pipes or thermosyphons. Int. J. Heat and Mass Transfer. 21:221-229.

Lee, Y., and V. Mital. 1972. A two-phase closed thermosyphon. INt. J. Heat Mass Transfer. 15(9):1695-1707.

Long, E.L. 1965. Means For Maintaining Permafrost Foundations. U.S. Patent 3,217,791. 7 pp.

Long, E.L., and E. Yarmack. 1982. Permafrost foundations maintained by passive refrigeration. ASME Pet. Div., Energy Sources Technology Conference and Exhibition, New Orleans, LA. 9 pp.

McDonnell Douglas Astronautics Co. 1974. Cyro-Anchor stabilizers -- refrigeration of arctic soils and foundation structures. Huntington Beach, CA. 14 pp.

McDonnell Douglas Corp. 1981. Cyro-Anchor performance and application summary. Huntington Beach, CA. MDC-G7529.

Meyers, G.E. 1971. Analytical methods in conduction heat transfer. McGraw-Hill, NY. p. 478.

Negishi, K., and T. Sawada. 1983. Heat transfer performance of an inclined two-phase closed thermosyphon. Int. J. Heat and Mass Transfer. 26(2):1207-1213.

Pearson, S.W. 1977. Thermal performance verification of thermal vertical support members for the Trans-Alaska pipeline. ASME Winter Annual Meeting, Atlanta, GA. ASME Paper 77-WA/HT-34.

Pekeris, C.L., and L.B. Slicher. 1939. Problem of ice formation. J. Appl. Phys. 10:135-137.

Perez, W. 1958. Thermal Pins. U.S. Patent 2,835,480. 9 pp.

Perkins, L.P., and W.E. Buck. 1892. Improvements in Devices for the Diffusion or Transference of Heat. U.K. Patent No. 22272. London.

Petrick, S.W. 1972. Hydrogen gas generation in water/stainless-heat pipes. Winter Annual Meeting, New York, NY. ASME Paper No. 72-WA/HT-37.

Reed, R.E. 1966. Refrigeration of a pipe pile by air circulation. U.S. Army CRREL, Hanover, NH. Tech. Report 156. 19 pp.

Reid, R.L., and A.L. Evans. 1983. Investigation of the air convection pile as a permafrost protection device. Pages 1048-1053 in Proceedings of 4th International Permafrost Conference. National Academy of Science, Washington, DC.

Reid, R.L., J.S. Tennant, and K.W. Childs. 1975. The modeling of a thermosyphon type permafrost protection device. AIAA/ASME Heat Transfer Conference, Boston, MA. ASME Paper No. 74-HT-46. 9 pp.

Sparrow, E.M., G.B. Miller and Johsson. 1962. Radiative effectiveness of annular-finned space radiators, including mutual irradiation between radiator elements. J. Aerospace Science. 29(11):1291-1299.

Swinbank, W.C. 1963. Long-wave radiation from clear skies. Quarterly Journal of the Royal Meteorological Society. Vol. 89.

Waters, E.D. 1973. Stabilization of soils and structures by passive heat transfer devices. Paper presented at 74th National Meeting of A.I.Ch.E., New Orleans.

Waters, E.D., C.L. Johnson and J.A. Wheeler. 1975. The application of heat pipes to the Trans-Alaska pipeline. 10th Intersociety Energy Conversion Engineering Conference, Newark, DE.

Yarmak, E. 1983. Personal communication. Arctic Foundations Inc., Anchorage, AK.

Zarling, J.P., and F.D. Haynes. 1984. Performance of a thermosyphon with an inclined evaporator and vertical condenser. Pages 64-68 in Proceedgins of the 3rd International Offshore Mechanics and Arctic Engineering Symposium, ASME.

Zarling, J.P., and F.D. Haynes. 1985. Laboratory tests and analysis of thermosyphons with inclined evaporator sections. Pages 31-37 in Proceedgins of the 4th International Offshore Mechanics and Arctic Engineering Symposium, ASME.